

A Dynamic Model for Double Bounded Time Series With Chaotic Driven Conditional Averages

Guilherme Pumi ^{a,*}, Taiane Schaedler Prass ^a and Rafael Rigão Souza ^a

Abstract

In this work we introduce a class of dynamic models for time series taking values on the unit interval. The proposed model follows a generalized linear model approach where the random component, conditioned on the past information, follows a beta distribution, while the conditional mean specification may include covariates and also an extra additive term given by the iteration of a map that can present chaotic behavior. This extra term can present a wide variety of behaviors including attracting and/or repelling fixed or periodic points, presence or absence of absolutely continuous invariant measure, etc. The resulting model is very flexible and its systematic component can accommodate short and long range dependence, periodic behavior, laminar phases, etc. We derive sufficient conditions for the stationarity of the proposed model, as well as conditions for the law of large numbers and a Birkhoff-type theorem to hold. We also discuss partial maximum likelihood inference and present some examples. A Monte Carlo simulation study is performed to assess the finite sample behavior of the proposed estimation procedure.

Keywords: time series; chaotic processes; generalized linear models.

2010 Mathematical Subject Classification: Primary: 37M10, 62M10, 62J12.

1 Introduction

Many time series encountered in statistical applications present two important characteristics: bounds, in the sense that its distribution has a bounded support, and serial dependence. Common cases are rates and proportions observed over time. In these cases, Gaussian based approaches are not adequate. Time series modeling of double bounded time series has been subject of intense research, especially in the last decade, and several approaches to the problem have been proposed. One such approach has received a lot of attention in the last few years. The idea is to include a time dependent structure into a generalized linear model (GLM) framework. The idea has been popularized in the works of Zeger and Qaqish (1988), Benjamin et al. (2003) and Ferrari and Cribari-Neto (2004) and processes that follow this type of structure are often referred to

^{*}Corresponding author. This Version: June 16, 2022

^aMathematics and Statistics Institute - Federal University of Rio Grande do Sul

E-mail: guilherme.pumi@ufrgs.br (G. Pumi), taiane.prass@ufrgs.br (T.S. Prass), rafars@mat.ufrgs.br (R.R. Souza)

as GARMA-like processes. More specifically, the model's systematic component follows the usual approach of GLM with an additional dynamic term of the form

$$g(\mu_t) = \eta_t = \mathbf{x}'_t \boldsymbol{\beta} + \tau_t, \quad (1)$$

where g is a suitable link function, μ_t is some quantity of interest (usually the (un)conditional mean or median), \mathbf{x}_t denotes a vector of covariates observed at time t and τ_t is a term responsible to accommodate any serial correlation in the sequence μ_t . The term τ_t can take a variety of forms, depending on the model's scope and intended application. In β ARMA models (Rocha and Cribari-Neto, 2009), for instance, the model's random component follows a (conditional) beta distribution while in the specification for the conditional mean μ_t , τ_t follows a classical ARMA process. In Bayer et al. (2017), the model's random component follows a (conditional) Kumaraswamy distribution while in the specification for the conditional median μ_t , τ_t also follows an ARMA process. Since ARMA models can only accommodate short range dependence, these models can only account for a short range dependence structure on their systematic component. In the case of conditionally beta distributed random component, Pumi et al. (2019) generalizes Rocha and Cribari-Neto (2009) by allowing τ_t to follow a long range dependent ARFIMA process (see, for instance, Honsking, 1981; Brockwell and Davis, 1991; Palma, 2007; Box et al., 2008). Inference for this type of models is done via partial maximum likelihood.

In this work we propose a model where the random component follows a conditional beta distribution, while the systematic component depends on the iterations of a (usually chaotic) map defined on the unit interval. Let $T : [0, 1] \rightarrow [0, 1]$ be a function of the interval $[0, 1]$ and let U_0 be a random variable taking values in $(0, 1)$. We consider the so-called class of chaotic process by setting $X_t := h(T^t(U_0))$, $t \in \mathbb{N}$, for a suitably smooth link function $h : (0, 1) \rightarrow \mathbb{R}$. Observe that T does not need to be a chaotic transformation in the usual sense (see next section) for X_t to be called a chaotic process. Such processes have been applied in a variety of problems from rock drilling (see Lasota and Yorke, 1973, and references therein) to intermittency in human cardiac rate (see Zebrowsky, 2001). Realizations of this type of process usually present complex dynamics, chaotic behavior and sensibility with respect to the initial point $u_0 = U_0(\omega)$ for ω in the sample space Ω . Figure 1(a) and (c) exemplifies the usual behavior of a chaotic map: even though the sample paths presented start only 0.01 apart of each other, after less than 10 steps the sample behavior of the processes are completely different.

The proposed model is mathematically advantageous compared to other GARMA-like processes presented in the literature. For instance, we obtain its covariance structure, simple conditions for stationarity, strong law of large numbers and also conditions for a Birkhoff-type theorem to hold. To the best of our knowledge, similar results are

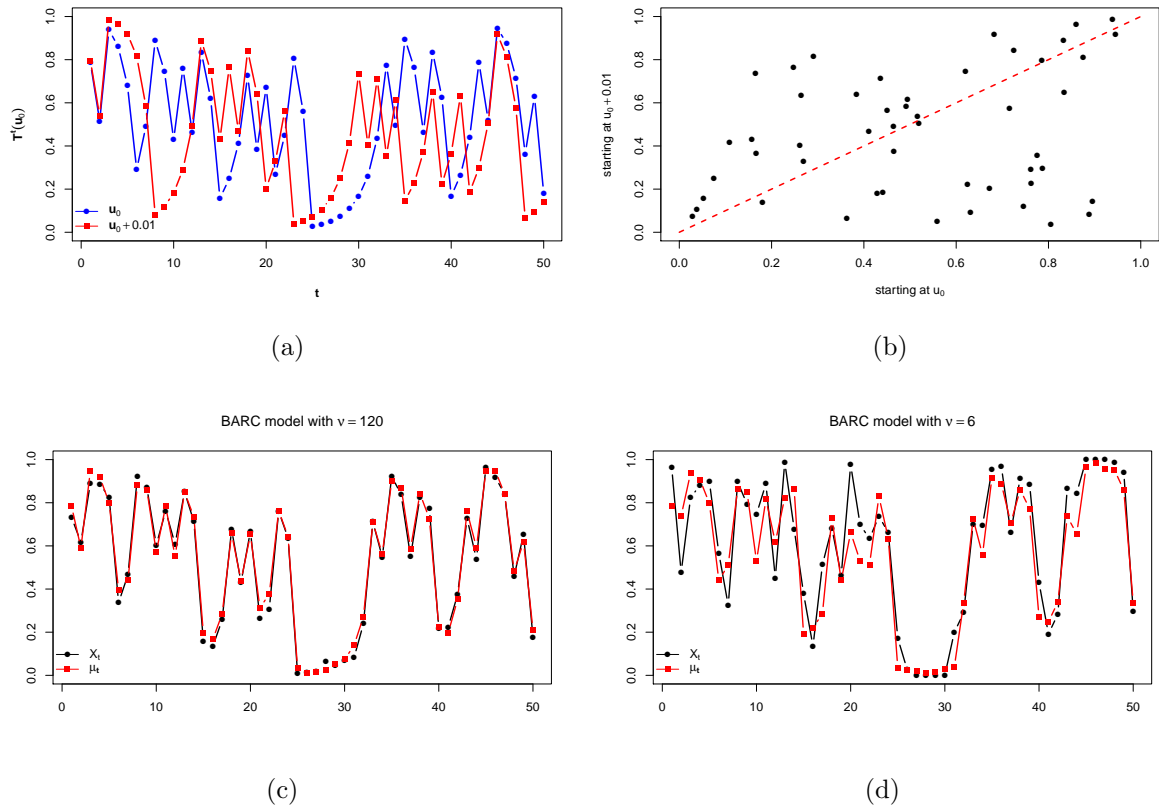


Figure 1: (a) Chaotic behavior of the Manneville-Pomeau transformation for parameter $s = 0.3$ starting at $u_0 = \pi/4$ (red) and $u_0 + 0.01$ (blue) and the associated scatter plot (b). (c) and (d) present the sample paths (black) and conditional mean μ_t (red) of two β ARC models obtained from the Manneville-Pomeau transformation starting at $u_0 = \pi/4$ with parameter $\phi_1 = 0.3$. In (c) we have $\nu = 6$ while in (d) $\nu = 120$.

not yet available even for the simplest cases of other GARMA-like processes presented in the literature, such as the β ARMA (Rocha and Cribari-Neto, 2009), KARMA (Bayer et al., 2017), β ARFIMA (Pumi et al., 2019), just to mention a few.

The paper is organized as follows. In the next section we define the model. In Section 3 we recall some standard definitions and examples of dynamical system, which are fundamental to proper motivate the model and understand some of the results of the following sections. In Section 4 we prove results related to stationarity and the law of large numbers. We also obtain conditions under which a Birkhoff-type theorem holds. In Section 5 we consider a partial maximum likelihood (PMLE) approach for parameter estimation for the proposed model. We also present a broad Monte Carlo simulation to assess the finite sample performance of the PMLE approach. The complete simulation results are presented in a supplementary material that accompanies the paper and an overview of the results is presented in Section 6. Conclusions are reserved to Section 7.

2 Model Definition

Let $\{Y_t\}_{t \geq 1}$ be a time series of interest and let $\{\mathbf{x}'_t\}_{t \geq 1}$ denote a set of l -dimensional exogenous time dependent (possibly random) covariates. Let \mathcal{F}_t denote the σ -field representing the observed history of the model up to time t , that is, the sigma-field generated by $(U_0, \mathbf{x}'_t, \dots, \mathbf{x}_1, Y_t, \dots, Y_1)'$, where U_0 will be a random variable of our interest. In this work we are concerned with an observation-driven model in which the random component follows a conditional beta distribution, parameterized as Ferrari and Cribari-Neto (2004):

$$f(y; \mu_t, \nu | \mathcal{F}_{t-1}) = \frac{\Gamma(\nu)}{\Gamma(\nu\mu_t)\Gamma(\nu(1-\mu_t))} y^{\nu\mu_t-1} (1-y)^{\nu(1-\mu_t)-1}, \quad (2)$$

for $0 < y < 1$, $0 < \mu_t < 1$ and $\nu > 0$, where $\mu_t := \mathbb{E}(Y_t | \mathcal{F}_{t-1})$. Observe that $\text{Var}(Y_t | \mathcal{F}_{t-1}) = \frac{\mu_t(1-\mu_t)}{1+\nu}$, so that ν acts as a precision parameter and that the model is conditionally heteroscedastic as the conditional variance depends on μ_t . Very high values of ν can account for conditional homoscedastic behavior in practice (this result is proven in Theorem 4.2). To define the systematic component of the proposed model, let $T_{\boldsymbol{\theta}} : [0, 1] \rightarrow [0, 1]$ be a function, potentially depending on an r -dimensional vector of parameters $\boldsymbol{\theta} = (\theta_1, \dots, \theta_r)' \in \mathbb{R}^r$, and $g, h : (0, 1) \rightarrow \mathbb{R}$ be two twice continuously differentiable link functions. In the additive specification (1) we consider τ_t as a process in the form

$$\eta_t := g(\mu_t) = \alpha + \mathbf{x}'_t \boldsymbol{\beta} + \sum_{j=1}^p \phi_j (g(y_{t-j}) - \mathbf{x}'_{t-j} \boldsymbol{\beta}) + h(T_{\boldsymbol{\theta}}^{t-1}(u_0)), \quad (3)$$

where $\alpha \in \mathbb{R}$ is an intercept, $\boldsymbol{\beta} := (\beta_1, \dots, \beta_l)'$ is an l -dimensional vector of parameter associated to the covariates, $\boldsymbol{\phi} := (\phi_1, \dots, \phi_p)'$ is a p -dimensional parameter related to the autoregressive structure in the model and $u_0 \in (0, 1)$ is a (fixed) initial point such that $T_{\boldsymbol{\theta}}^t(u_0) \in (0, 1)$, for all t . Specification (2) and (3) define the proposed model, which we shall call beta autoregressive chaotic of order p and denote by $\beta\text{ARC}(p)$ models.

In the absence of covariates and autoregressive parts, the behavior of μ_t often defines the overall behavior of the associated sample path, as exemplified in Figure 1(b). This means that the richness of possible sample paths in the class of all possible process can also be translated directly into the context of βARC models. Hence, the most interesting case of the proposed model occurs in the absence of covariates and the autoregressive parts. In that case, the canonical link is adequate and the conditional average μ_t is driven solely by the behavior of the transformation $T_{\boldsymbol{\theta}}$ with the model's

systematic component simplifying to

$$\mu_t = T_{\theta}^{t-1}(u_0). \quad (4)$$

In what follows we shall refer to the β ARC model following (4) as pure chaotic β ARC models. As we shall see in the next sections, for almost all $u_0 \in (0, 1)$, $T_{\theta}^t(u_0) \in (0, 1)$, for all t , with probability 1, so that (4) is well defined (the underlying probability measures will be discussed later). Some interesting simple results for pure β ARC models are presented in Proposition 2.1. One of them show that the covariance structure of the dynamics $\{\mu_t\}_{t \geq 1}$ ultimately determines the covariance structure of the process $\{Y_t\}_{t \geq 1}$, unconditionally. To the best of our knowledge, similar results are not available for any other competing GARMA-like processes in the literature.

Proposition 2.1. *Let $\{Y_t\}_{t \geq 1}$ be a pure β ARC process following (4). Then, for all $t, h > 0$,*

- (a) $\mathbb{E}(Y_t) = \mathbb{E}(\mu_t)$.
- (b) $\text{Var}(Y_t) = \text{Var}(\mu_t) + \frac{1}{1 + \nu} \mathbb{E}(\mu_t(1 - \mu_t))$.
- (c) $\text{Cov}(Y_t, Y_{t+h}) = \text{Cov}(\mu_t, \mu_{t+h})$.

Proof: Item (a) follows from $\mathbb{E}(Y_t) = \mathbb{E}(\mathbb{E}(Y_t | \mathcal{F}_{t-1})) = \mathbb{E}(\mu_t)$, while (b) follows from the identity $\text{Var}(Y_t) = \text{Var}(\mathbb{E}(Y_t | \mathcal{F}_{t-1})) + \mathbb{E}(\text{Var}(Y_t | \mathcal{F}_{t-1}))$ and (a). As for (c), for any $t, h > 0$, from item (a) we obtain

$$\text{Cov}(Y_t, Y_{t+h}) = \mathbb{E}(Y_t Y_{t+h}) - \mathbb{E}(Y_t) \mathbb{E}(Y_{t+h}) = \mathbb{E}(Y_t Y_{t+h}) - \mathbb{E}(\mu_t) \mathbb{E}(\mu_{t+h}). \quad (5)$$

Now, notice that μ_t is \mathcal{F}_1 -measurable, for all $t > 0$, so that

$$\begin{aligned} \mathbb{E}(Y_t Y_{t+h}) &= \mathbb{E}(\mathbb{E}(Y_t Y_{t+h} | \mathcal{F}_{t+h-1})) = \mathbb{E}(Y_t \mathbb{E}(Y_{t+h} | \mathcal{F}_{t+h-1})) = \mathbb{E}(Y_t \mu_{t+h}) \\ &= \mathbb{E}(\mathbb{E}(Y_t \mu_{t+h} | \mathcal{F}_{t-1})) = \mathbb{E}(\mu_{t+h} \mathbb{E}(Y_t | \mathcal{F}_{t-1})) = \mathbb{E}(\mu_t \mu_{t+h}), \end{aligned} \quad (6)$$

and the result follows upon replacing (6) into (5). ■

3 Statistical Properties of Dynamical Systems

The proposed β ARC models strongly rely on the dynamic T_{θ} . For instance, in view of Proposition 2.1, the knowledge of the covariance decay of the dynamical system will translate vis-à-vis to the covariance decay of the process itself. For this reason, in order

to explore the richness of behaviors that can be observed under specification (4), in this section we introduce some examples of one dimensional dynamic systems (ODDS) defined on the interval $[0, 1]$.

Before we proceed we introduce some standard definitions and results in discrete dynamical systems, beginning by some measure oriented definitions (i.e. from ergodic theory) and following by topological ones (from standard one dimensional dynamical systems). As general and very comprehensive references for ergodic theory we have Hasselblatt and Katok (1996) and Walters (1982), while for topological aspects we refer the reader to Devaney (2003); Robinson (1998).

Let $T : [0, 1] \rightarrow [0, 1]$ be a Borel measurable transformation. λ_T is called a T -invariant probability measure (or invariant measure for short) if λ_T is a probability measure defined on the Borel sets of $[0, 1]$ which satisfies $\lambda_T(T^{-1}(A)) = \lambda_T(A)$ for all measurable set $A \subset [0, 1]$. If such invariant measure is absolutely continuous with respect to the Lebesgue measure, then we call it an ACIM. An invariant measure λ_T is called ergodic if the only measurable sets that are invariant for T are sets of full or zero measure, i.e., if $T^{-1}(A) = A$ implies $\lambda_T(A) = 0$ or $\lambda_T(A) = 1$ (ergodicity implies that it is not possible to split the dynamics into two invariant sets with both having nonzero measure).

Birkhoff Ergodic Theorem states that, if λ_T is ergodic for T , then for any λ_T -integrable function $f : [0, 1] \rightarrow \mathbb{R}$, and for λ_T -almost all $x \in [0, 1]$, we have

$$\lim_{n \rightarrow \infty} \frac{1}{n} \sum_{k=0}^{n-1} f(T^k(x)) = \int_0^1 f d\lambda_T.$$

In particular, by taking $f(x) = I_A(x)$, the indicator of A , Birkhoff's theorem implies the convergence of the histogram (that is, the sample density) to the associated density (Ding and Zhou, 2009).

Given a transformation T , the sequence of iterates $\{x_0, x_1, x_2, \dots\}$, where $x_{k+1} = T(x_k)$, is called the orbit of x_0 . A point x is called a fixed point if $T(x) = x$ and it is called a periodic point with period s (where s is a positive integer) if $T^s(x) = x$ and $T^k(x) \neq x$, for all $k < s$. Any continuous transformation $T : [a, b] \rightarrow [a, b]$ has at least one fixed point. Fixed and periodic points can be very different in its nature, as we will see in the next paragraphs, and are related to the presence or absence of ACIM. If T is differentiable at a fixed point x we say that x is attracting if $|T'(x)| < 1$, repelling if $|T'(x)| > 1$, and indifferent (or neutral) if $|T'(x)| = 1$. If there exists an open interval I containing x such that, for any $y \in I \setminus \{x\}$, $T^k(y) \rightarrow x$ when $k \rightarrow \infty$, then x is called weakly attracting. On the other side, we say that x is weakly repelling if there exists

an open interval I containing x such that, for any $y \in I \setminus \{x\}$, there exists a k satisfying $T^k(y) \notin I$. Note that an attracting fixed point is weakly attracting and a repelling fixed point is weakly repelling. An indifferent fixed point can be weakly attracting, weakly repelling, or has a mixed behaviour where it exists a small neighborhood of the point such that points on one side of this neighborhood are attracted and points on the other side are repelled. Points near a repelling fixed point are pushed away after some iterations of the map, and the subsequent behavior depends on the global properties of the function. Sometimes the sequence of iterates of a repelling fixed point can come back to a neighborhood of this point after some iterations.

We also say that a periodic point x of period s is attracting (respectively repelling or indifferent) if $|(T^s)'(x)| < 1$ (resp. $|(T^s)'(x)| > 1$ or $|(T^s)'(x)| = 1$). Analogously we can talk about weakly attracting or weakly repelling periodic points. Figure 2 shows the graph of the map $T(x) = \theta x(1 - x)$, for $\theta = 2.5$ and 3.5 and the first three elements of the orbit of $x_0 = 0.3$ and 0.7 , respectively. The diagonal $y = x$ is included to help drawing the orbit of x_0 . Figure 2(a) shows that the orbit approaches the attracting fixed point $p = 0.6$. The fact that $|T'(p)| < 1$ makes p an attracting fixed point and the negative sign of the derivative at p makes the orbit oscillate around p , while converging to p . In contrast, Figure 2(b) pictures the behavior of the map near a repelling fixed point.

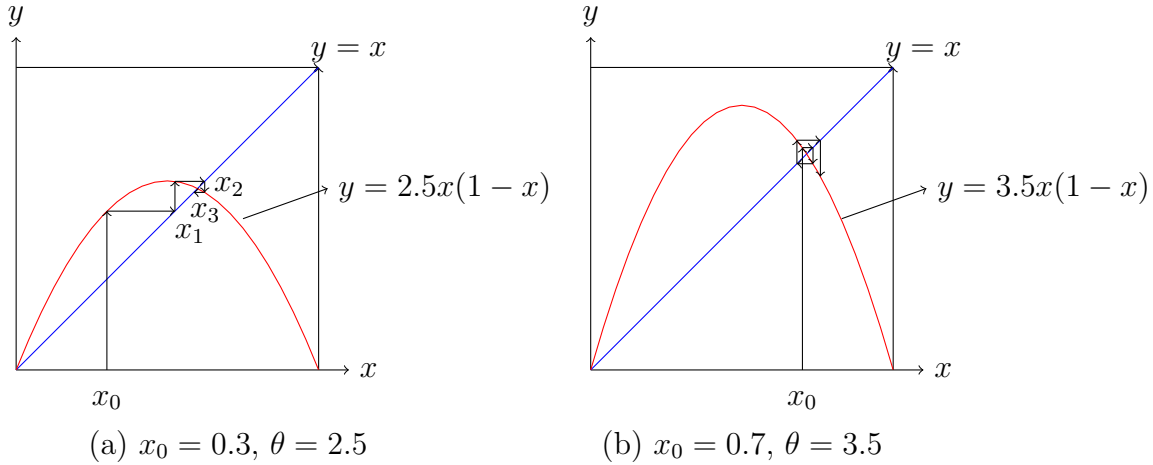


Figure 2: The first three elements of the orbit of x_0 for the map $T(x) = \theta x(1 - x)$. In (a) $p = 0.6$ is an attracting fixed point while in (b) $p = 5/7$ is a repelling fixed point.

An important case where all the fixed or periodic points are repelling is given by the uniformly expanding maps: we say that T is uniformly expanding if T is continuously differentiable and there exists $\rho > 1$ such that $|T'(x)| \geq \rho$, for all $x \in (0, 1)$. This kind of maps are also called *hyperbolic maps*. Any fixed point of an uniformly expanding map is repelling. Also, if we require the derivative of such maps to be Hölder-continuous, then they present an unique ACIM, which gives positive mass to any open subset, and

is also ergodic (see Boyarsky and Gora, 1997; Hasselblatt and Katok, 1996; de Melo and Van Strien, 1993, and references therein). This remarkable feature do not occur in maps that present attracting fixed or periodic points.

Before passing to some examples of maps we will use in the β ARC model, we present, for completeness, the traditional definition of a chaotic map. A map is called chaotic if it satisfies the following three conditions: (i) it is sensitive to initial conditions; (ii) it is topologically transitive and (iii) it has dense periodic orbits. The first condition is the most interesting one, and it is usually easy to verify. For instance, the presence of attracting fixed or periodic points implies the map is not chaotic, as first condition is clearly not possible under this hypothesis (we remark the fact that the dense periodic orbits required by the third item above are repelling ones). In the sequel we present 4 examples of maps displaying several interesting behaviors. Maps 1 and 2 are examples of chaotic maps, as well as map 4, while map 3 can be chaotic or not, depending on the parameter θ . We observe, however, that a deep understanding of the three conditions above is not required to what follows so that we refrain for further discussion on the subject. For more details see Devaney (2003).

Map 1. One of the simplest ODDS is the map defined by

$$T_k(x) = (kx) \pmod{1},$$

where k is a natural number greater or equal to 2. Figure 3(a) presents this function for $k = 3$. It is the basic model of hyperbolic, uniformly expanding map, presenting a simpler ACIM: the Lebesgue probability measure. As a consequence of the Birkhoff's theorem, if we take any point in a set of total Lebesgue measure in $[0, 1]$, then the orbit $\{T^t(U_0)\}_{t \geq 0}$ will be dense on the unit interval, and the histogram of a size n sample from this orbit will converge to the constant function, as n increases. Although there exists periodic points of any period for this maps, all the periodic points are obviously repelling and the set of such points is countable, and therefore has zero Lebesgue measure.

Map 2. The second example is the map

$$T_\theta(x) = \begin{cases} \frac{x}{\theta} & \text{if } 0 \leq x < \theta, \\ \frac{\theta(x-\theta)}{1-\theta} & \text{if } \theta \leq x \leq 1. \end{cases} \quad (7)$$

In Figure 4(a) we present a plot from this transformation for $\theta = 0.4$. Depending on the parameter θ this map can be expanding or not, but its second iterate is always expanding. Therefore, this map also have an ACIM that can be explicitly calculated (see Lopes et al., 1996) and is given by the invariant density $f_\theta(x) = (2 - \theta)^{-1} \theta^{-I(x < \theta)}$

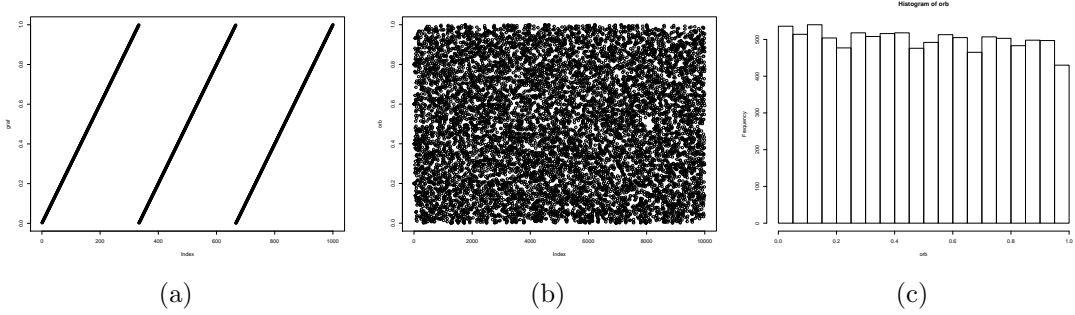


Figure 3: (a) The map $T(x) = 3x(\text{mod } 1)$ (b) Sample path of this map for $u_0 = \pi/10$: the absence of attracting fixed or periodic points makes possible the chaotic behavior of this map (c) Histogram of the first 10,000 iterates of the map.

which can be recovered in the histogram of the orbit, for large samples (see Figure 4(b) and (c)).

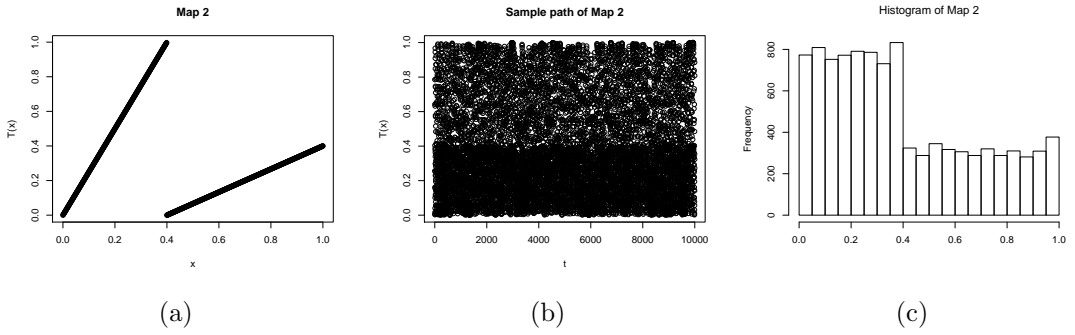


Figure 4: (a) A plot of the map given by (7) for $\theta = 0.4$. (b) Sample path of this map for $u_0 = \pi/4$. (c) Histogram of the first 10,000 iterates of the map.

Map 3. For $0 \leq \theta \leq 4$, the Logistic map³ is given by

$$T_\theta(x) = \theta x(1 - x).$$

This map is not expanding: in fact it has derivative zero on $x = 1/2$. Therefore, its analysis is more complicated than the preceding examples: we can observe different behaviors for the Logistic map, depending on the parameter θ . For $\theta < 3$ the Logistic map has an attracting fixed point, as can be seen in Figure 2. The most interesting behaviors occurs for $\theta > 3$. As it can be seen in Figure 5, the fixed points are both repellors, as the derivative has modulus greater than 1. For $\theta = 10/3$ the logistic map has an attracting periodic orbit of period 2, shown in Figure 6(a). For $\theta = 4$ the Logistic map has no attracting periodic points, which allows very complicated sample paths (Figure 6(b)), and has an ACIM which can be seen in Figure 6(c). Figure 7(a)-(i)

³also called *quadratic family*

present some sample paths of the Logistic Map for θ going from 3.55 to 3.95. For more information on the Logistic map, see Devaney (2003); Robinson (1998).

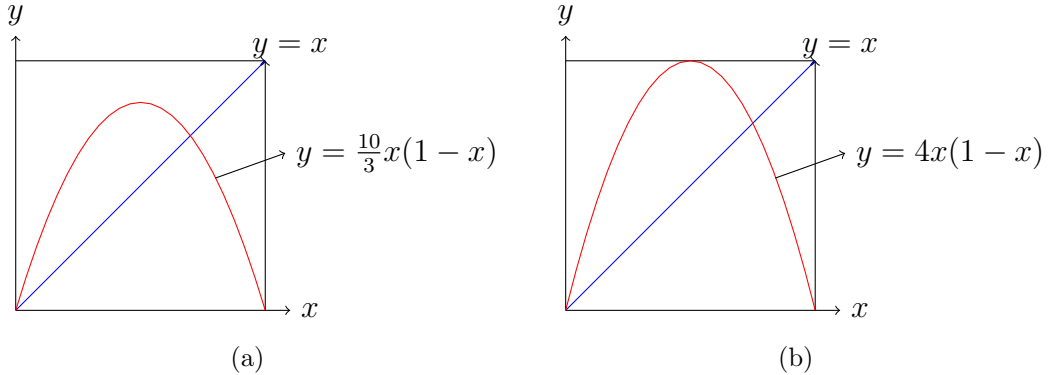


Figure 5: (a) The logistic map for $\theta = 10/3$. (b) The logistic map for $\theta = 4$.

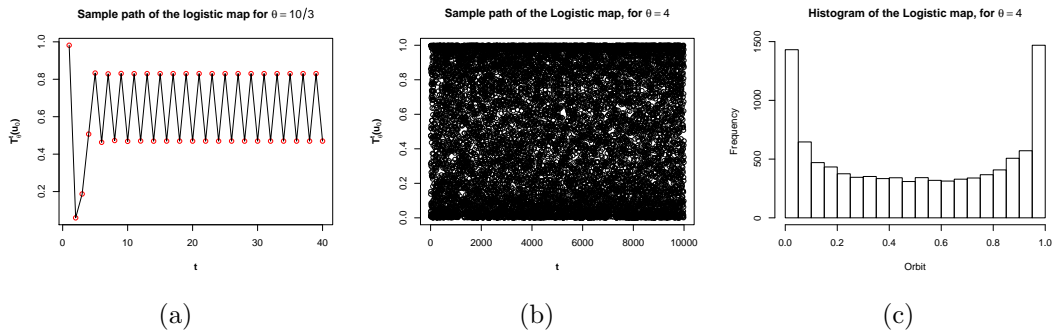


Figure 6: (a) Plot of a sample path associated to the logistic map for $\theta = 10/3$ starting at $u_0 = \pi/3.2$ showing an attracting periodic orbit of period 2; (b) sample path of the logistic map for $\theta = 4$; (c) Histogram of the sample path in (b).

Map 4. Now we present a family of maps presenting and indifferent fixed on $x = 0$, that can have or not an ACIM depending on the parameter chosed. For $s > 0$, the Manneville-Pomeau transformation $T_s : [0, 1] \rightarrow [0, 1]$, is given by

$$T_s(x) = (x + x^{1+s}) \pmod{1}. \quad (8)$$

Figure 8(a) show the Manneville-Pomeau transformation for $s = 0.75$. The Manneville-Pomeau transformation presents a property referred to as transition to turbulence through intermittency (Eckmann, 1981). For $s \in (0, 1)$, there exists an absolutely continuous T_s -invariant probability measure (Thaler, 1980), which can be seen in Figure 8(c). The Manneville-Pomeau transformation has an indifferent fixed point at 0 and, hence, it is not uniformly expanding. The chaotic processes associated to T_s are often called Manneville-Pomeau processes which present a very slow correlation decay when $s \in (0.5, 1)$, characteristic of long range dependent processes and it is commonly

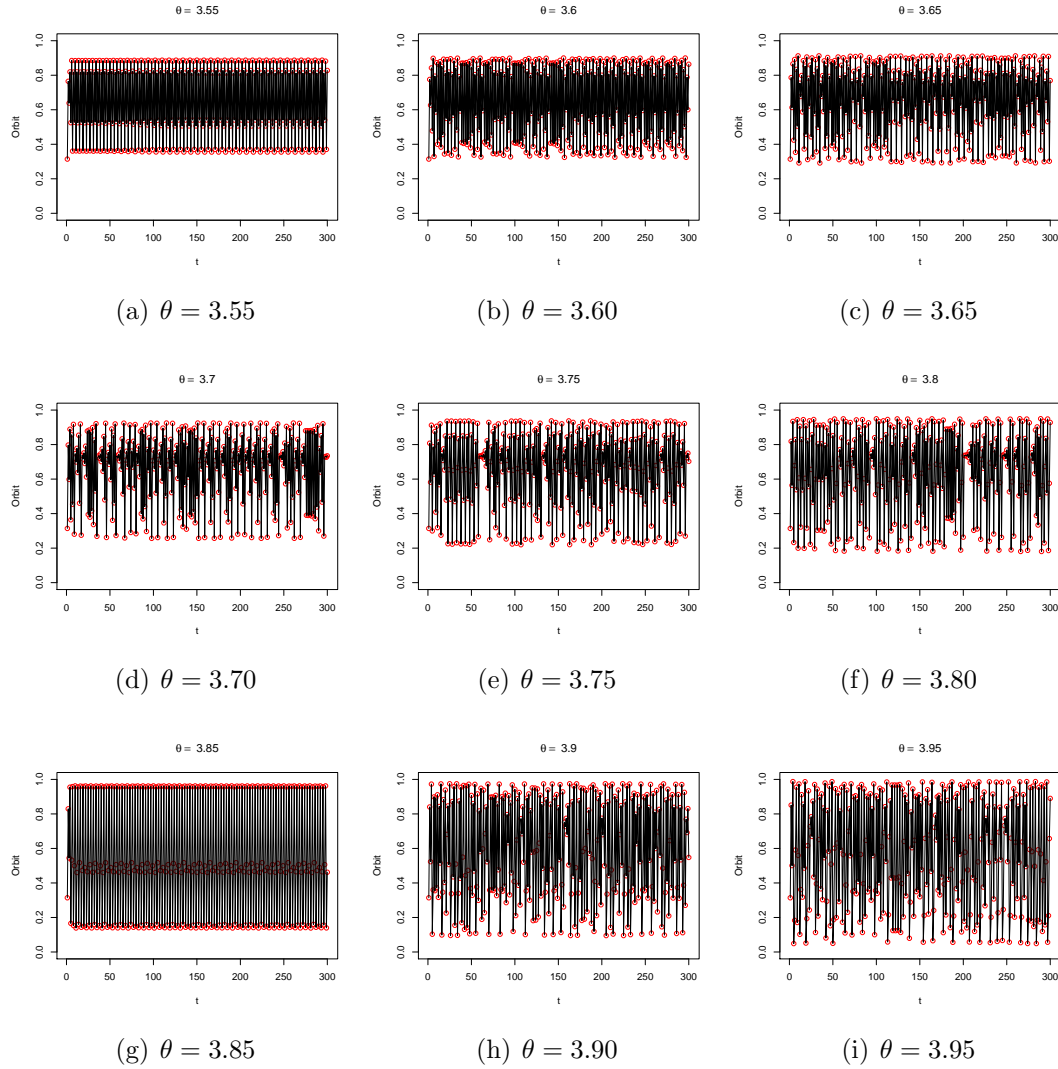


Figure 7: Sample paths of the logistic map for θ from 3.55 to 3.95 with $u_0 = \pi/10$.

viewed as an alternative model for long range dependence outside the classical duet of Fractional Brownian Motion and ARFIMA processes. This slow decay is mainly due to the presence of laminar behavior near zero, which can be seen in Figure 8(b).

4 Stationarity of the β ARC processes

Conditions for stationarity of dynamical models for time series following a GARMA approach are traditionally very hard to obtain and remain an open subject in most traditional models, such as β ARMA (Rocha and Cribari-Neto, 2009), β ARFIMA (Pumi et al., 2019) and KARMA models (Bayer et al., 2017) except in very simple scenarios. In this section we shall show that the pure chaotic β ARC models are stationary in a very broad specification and under easily verifiable conditions.

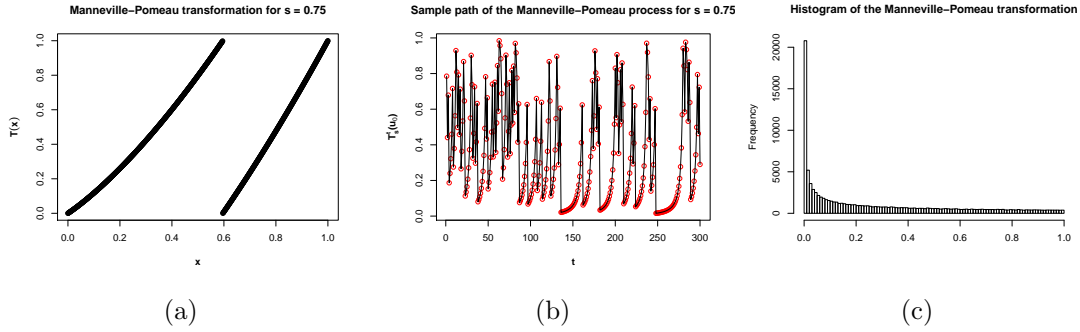


Figure 8: (a) A plot of the Manneville-Pomeau transformation (8) for $s = 0.75$. (b) Sample path of this map for $u_0 = \pi/4$ showing laminar behavior near zero. (c) Histogram of the first 100,000 iterates of the map.

Theorem 4.1. Let $\{Y_t\}_{t \geq 1}$ be a β ARC model with $\nu > 0$ and

$$\eta_t = g(\mu_t) = \alpha + \mathbf{x}'_t \boldsymbol{\beta} + h(T_{\boldsymbol{\theta}}^{t-1}(u_0)),$$

where $\{\mathbf{x}_t\}_{t \geq 1}$ is a set of random covariates, g and h are twice continuously differentiable, one to one link functions, $u_0 \in (0, 1)$ is such that the trajectories $T_{\boldsymbol{\theta}}^t(u_0) \in (0, 1)$ for all t . Then $\{(Y_t, \mu_t)\}_{t \geq 1}$ is jointly stationary if and only if $\{\mu_t\}_{t \geq 1}$ is stationary.

Proof: Suppose that $\{\mu_t\}_{t \geq 1}$ is stationary. For any arbitrary positive integer k , let t_1, \dots, t_k be distinct time points, $\mathbf{t} = (t_1, \dots, t_k)$, $\mathbf{t} + h = (t_1 + h, \dots, t_k + h)$, $\mathbf{Y}_t = (Y_{t_1}, \dots, Y_{t_k})$ and $\boldsymbol{\mu}_t = (\mu_{t_1}, \dots, \mu_{t_k})$. Using Riemann-Stieltjes integration we have

$$F_{Y_t|\mu_t}(y|z) = P(Y_t \leq y | \mu_t = z) = \int_0^y dF_{Y_t|\mu_t}(u|z), \quad \forall y, z \in (0, 1),$$

$$F_{\boldsymbol{\mu}_t}(v_1, \dots, v_k) = P(\mu_{t_1} \leq v_1, \dots, \mu_{t_k} \leq v_k) = \int_0^{v_1} \cdots \int_0^{v_k} dF_{\boldsymbol{\mu}_t}(z_1, \dots, z_k)$$

and

$$\begin{aligned} F_{\mathbf{Y}_t, \boldsymbol{\mu}_t}(u_1, \dots, u_k, v_1, \dots, v_k) &= P(Y_{t_1} \leq u_1, \dots, Y_{t_k} \leq u_k, \mu_{t_1} \leq v_1, \dots, \mu_{t_k} \leq v_k) \\ &= \int_0^{u_1} \cdots \int_0^{u_k} \int_0^{v_1} \cdots \int_0^{v_k} dF_{\mathbf{Y}_t, \boldsymbol{\mu}_t}(y_1, \dots, y_k, z_1, \dots, z_k), \end{aligned}$$

for all $u_1, \dots, u_k, v_1, \dots, v_k \in (0, 1)$, where dF_{Y_t, μ_t} , $dF_{\boldsymbol{\mu}_t}$ and $dF_{\mathbf{Y}_t, \boldsymbol{\mu}_t}$ are the integrands of the Riemann-Stieltjes integrals. Observe that, for all $t > 0$, given $\mu_t = z$, the random variable Y_t depends, neither on the past information $\{Y_s, \mu_s\}_{s < t}$, nor on the future μ_s ,

$s > t$, so that

$$dF_{Y_t, \mu_t}(y_1, \dots, y_k, z_1, \dots, z_k) = dF_{\mu_t}(z_1, \dots, z_k) \prod_{j=1}^k dF_{Y_{t_j} | \mu_{t_j}}(y_j | z_j).$$

It is easy to see that $dF_{Y_t | \mu_t}(y | z) = f(y; z, \nu | \mathcal{F}_{t-1}) dy$, where f is the conditional density defined by (2) and that $dF_{Y_t | \mu_t}(y | z) = dF_{Y_1 | \mu_1}(y | z) = dF_{Y_{t+h} | \mu_{t+h}}(y | z)$, for all $t, h > 0$, so that, from the stationarity of $\{\mu_t\}_{t \geq 1}$, it follows that, for all $A_i, B_i \subset (0, 1)$, $i = 1, \dots, k$,

$$\begin{aligned} P(Y_{t_1} \in A_1, \dots, Y_{t_k} \in A_k, \mu_{t_1} \in B_1, \dots, \mu_{t_k} \in B_k) &= \\ &= \int_{A_1} \dots \int_{A_k} \int_{B_1} \dots \int_{B_k} dF_{Y_t, \mu_t}(y_1, \dots, y_k, z_1, \dots, z_k) \\ &= \int_{A_1} \dots \int_{A_k} \int_{B_1} \dots \int_{B_k} dF_{\mu_t}(z_1, \dots, z_k) \prod_{j=1}^k dF_{Y_{t_j} | \mu_{t_j}}(y_j | z_j) \\ &= \int_{A_1} \dots \int_{A_k} \int_{B_1} \dots \int_{B_k} dF_{\mu_{t+h}}(z_1, \dots, z_k) \prod_{j=1}^k dF_{Y_{t_j+h} | \mu_{t_j+h}}(y_j | z_j) \\ &= P(Y_{t_1+h} \in A_1, \dots, Y_{t_k+h} \in A_k, \mu_{t_1+h} \in B_1, \dots, \mu_{t_k+h} \in B_k). \end{aligned}$$

This implies that $\{(Y_t, \mu_t)\}_{t \geq 1}$ is jointly stationary. The converse is obvious. \blacksquare

Corollary 4.1. *Under the conditions of Theorem 4.1, if $\{\mu_t\}_{t \geq 1}$ is stationary, then so is $\{Y_t\}_{t \geq 1}$.*

Proof: Observe that, if $\{\mu_t\}_{t \geq 1}$ is stationary then from Theorem 4.1 $\{(Y_t, \mu_t)\}_{t \geq 1}$ is jointly stationary and hence, $\{Y_t\}_{t \geq 1}$ is stationary. \blacksquare

Corollary 4.2. *Let T_θ be a dynamical system with ACIM given by λ_T and let $\{Y_t\}_{t \geq 1}$ be a pure chaotic β ARC model with $\nu > 0$ where $\mu_t = T_\theta^{t-1}(u_0)$ and u_0 is chosen accordingly to λ_T . Then $\{Y_t\}_{t \geq 1}$ is stationary and the common marginal distribution F_{Y_t} is absolutely continuous with respect to the Lebesgue measure, with unconditional density given by*

$$f_{Y_t}(y) = \int_0^1 f_{Y_t | \mu_t}(y | z) \lambda_T(dz),$$

where $f_{Y_t | \mu_t}(y | z) = f(y; z, \nu | \mathcal{F}_{t-1})$ is the conditional density of Y_t given μ_t , defined by (2).

Proof: The stationarity of $\{Y_t\}_{t \geq 1}$ follows immediately from Corollary 4.1, as μ_t is clearly stationary in this case. Now, let f_{Y_t, μ_t} denote the joint density of (Y_t, μ_t) , so we have

$$f_{Y_t}(y) = \int_0^1 f_{Y_t, \mu_t}(y, z) dz = \int_0^1 f_{Y_t | \mu_t}(y | z) \lambda_T(dz),$$

and the proof is complete ■.

Corollary 4.3. *Let T_{θ} be a dynamical system with ACIM given by λ_T , $\{\mathbf{x}_t\}_{t \geq 1}$ be a set of random covariates. Let $\{Y_t\}_{t \geq 1}$ be a β ARC model with $\nu > 0$ for $u_0 \in (0, 1)$ obtained from λ_T and with*

$$\eta_t = g(\mu_t) = \alpha + \mathbf{x}'_t \boldsymbol{\beta} + h(T_{\theta}^{t-1}(u_0)),$$

for two twice continuously differentiable, one to one link functions g and h . Then if $\{\mathbf{x}_t\}_{t \geq 1}$ is stationary, so is $\{Y_t\}_{t \geq 1}$.

Proof: Since g and h are both measurable functions, $\{\mu_t\}_{t \geq 1}$ is stationary if and only if $\{\mathbf{x}_t\}_{t \geq 1}$ is stationary and the result follows immediately from Theorem 4.1. ■

Remark 4.1. The proof of Theorem 4.1 is also valid under the full specification (3). However, verification of the hypothesis under (3) is difficult since it is not presented in an autoregressive fashion as we write η_t in terms of past values of Y_t and \mathbf{x}_t , which depends on the past of η_t in a non-trivial way. In this scenario it is challenging to obtain stationarity conditions for $\{\eta_t\}_{t \geq 1}$ under the full specification (3). This and the recursive nature of μ_t for similar GARMA-like models, such as the β ARMA, β ARFIMA and KARMA, make obtaining stationarity conditions a non-trivial problem for these models.

The first example we shall analyze is the stationarity of the β ARC model with $T(x) = (kx) \text{mod}(1)$ for an integer $k > 0$. In this case, the Lebesgue measure in $[0, 1]$ is T invariant and the unconditional distribution of Y_t is given by

$$f_{Y_t}(x) = \frac{\Gamma(\nu)(1-x)^{\nu-1}}{x} \int_0^1 \left[\frac{x}{1-z} \right]^{\nu z} \frac{1}{\Gamma(\nu z) \Gamma(\nu(1-z))} dz.$$

The behavior of f_{Y_t} depends on the magnitude of ν . In Figure 9 we show the behavior for several values of ν .

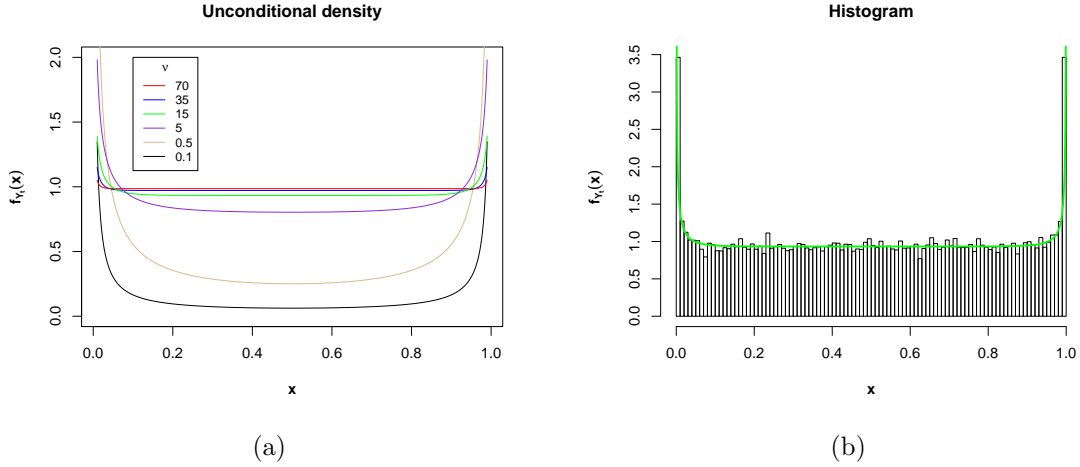


Figure 9: (a) The unconditional density of the pure β ARC model with $T(x) = (kx)\text{mod}(1)$ and (b) histogram of an associated sample of size $n = 30,000$ starting at $u_0 = \pi/4$, with $\nu = 15$.

Now consider the pure β ARC coupled with Map 2. For any $\theta \in (0, 1)$, the unconditional distribution of Y_t is given by

$$f_{Y_t}(x) = \frac{\Gamma(\nu)(1-x)^{\nu-1}}{x} \left(\int_0^x \left[\frac{x}{1-x} \right]^{\nu z} \frac{1}{(2-z)\Gamma(\nu z)\Gamma(\nu(1-z))} dz + \int_x^1 \left[\frac{x}{1-x} \right]^{\nu z} \frac{1}{z(2-z)\Gamma(\nu z)\Gamma(\nu(1-z))} dz \right).$$

In Figure 10 we show the behavior of f_{Y_t} for several values of ν .

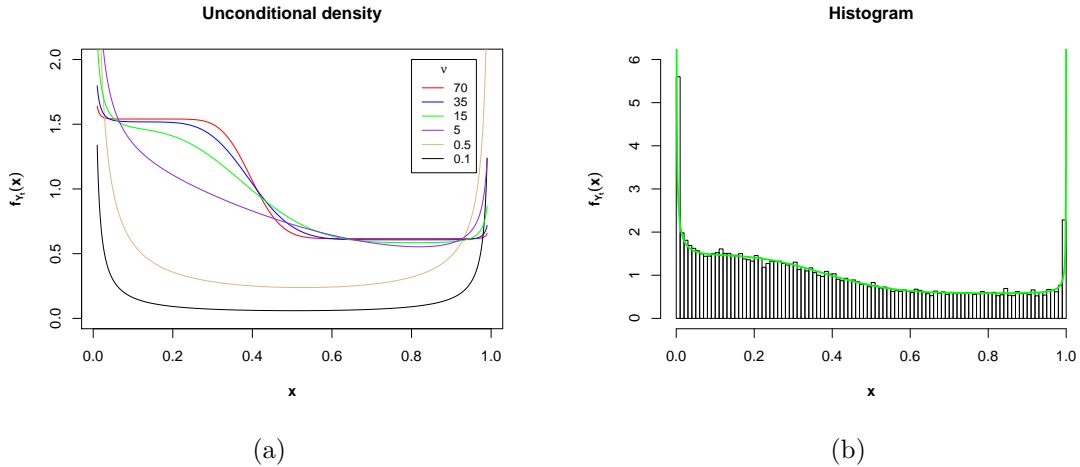


Figure 10: (a) The unconditional density of the pure β ARC model for Map 2 and (b) histogram of an associated sample of size $n = 30,000$ starting at $u_0 = \pi/4$, with $\nu = 15$.

The next two theorems present general results for β ARC processes that do not require stationarity assumptions. The first one shows that, as the precision parameter

increases, the closer the β ARC model resembles its conditional mean.

Theorem 4.2. *Let $\{Y_t\}_{t \geq 1}$ be a β ARC process. Then, for each fixed $t > 0$,*

$$Y_t \xrightarrow{d} \mu_t, \quad \text{as } \nu \rightarrow \infty.$$

Proof: First, for fixed $t > 0$, observe that $\text{Var}(Y_t | \mathcal{F}_{t-1}) = \frac{\mu_t(1-\mu_t)}{1+\nu} \rightarrow 0$ as $\nu \rightarrow \infty$ so that,

$$P\left(\left\{\omega : Y_t(\omega) \xrightarrow{\nu \rightarrow \infty} \mathbb{E}(Y_t | \mathcal{F}_{t-1})(\omega)\right\} | \mathcal{F}_{t-1}\right) = 1.$$

Now we can also use the fact that $\mathbb{E}(Y_t | \mathcal{F}_{t-1}) = \mu_t$ to conclude that, for any $0 < c < 1$ which is a continuity point of F_{μ_t} , we have

$$P(Y_t \leq c | \mu_t = z) \rightarrow \begin{cases} 1 & \text{if } c > z, \\ 0 & \text{if } c < z, \end{cases}$$

when $\nu \rightarrow \infty$. Therefore,

$$P(Y_t \leq c) = \int_0^1 P(Y_t \leq c | \mu_t = z) dF_{\mu_t}(z) \rightarrow \int_0^c 1 dF_{\mu_t}(z) = P(\mu_t \leq c)$$

when $\nu \rightarrow \infty$, by the Lebesgue dominated convergence theorem. \blacksquare

The next theorem presents a simple condition under which the strong law of large numbers holds for β ARC process. In particular, for a stationary β ARC process, the strong law of large numbers for $\{Y_t\}_{t \geq 1}$ is related to the covariance structure of the dynamical system $\{\mu_t\}_{t \geq 1}$.

Theorem 4.3. *Let $\{Y_t\}_{t \geq 1}$ be a β ARC process and $\varphi : [0, 1] \rightarrow \mathbb{R}$ be a measurable function such that $\mathbb{E}(\varphi(Y_t)^2) < \infty$, for all $t > 0$. If*

$$\sum_{k=1}^{\infty} \frac{\sup_{t \geq 1} \{|\text{Cov}(\varphi(Y_t), \varphi(Y_{t+k}))|\}}{k^q} < \infty, \quad \text{for some } 0 \leq q < 1, \quad (9)$$

and

$$\sum_{k=1}^{\infty} \frac{\text{Var}(\varphi(Y_k)) \ln(k)^2}{n^2} < \infty \quad (10)$$

then

$$\lim_{n \rightarrow \infty} \frac{1}{n} \sum_{\ell=0}^{n-1} [\varphi(Y_\ell) - \mathbb{E}(\varphi(Y_\ell))] = 0, \quad \text{a.s.} \quad (11)$$

Proof: The result follows from theorem 1 in Hu et al. (2008). \blacksquare

Remark 4.2. Observe that if $\{Y_t\}_{t \geq 1}$ is stationary, so is $\{\varphi(Y_t)\}_{t > 0}$, hence (10) is

always satisfied and condition (9) becomes

$$\sum_{k=1}^{\infty} \frac{|\text{Cov}(\varphi(Y_t), \varphi(Y_{t+k}))|}{k^q} < \infty, \quad \text{for some } 0 \leq q < 1.$$

Moreover, in this case the conclusion is a Birkhoff-type theorem since (11) becomes

$$\lim_{n \rightarrow \infty} \frac{1}{n} \sum_{\ell=0}^{n-1} \varphi(Y_\ell) = \int \varphi(z) dF_{Y_t}(z) \quad \text{a.s.}$$

Remark 4.3. An interesting corollary to Theorem 4.3 is obtained by taking φ as the identity function. In view of Proposition 2.1 and Corollary 4.1, for a pure β ARC associated to a dynamical system presenting ACIM λ_T , a sufficient condition for (9) to hold is

$$\sum_{k=1}^{\infty} \frac{|\text{Cov}(\mu_t, \mu_{t+k})|}{k^q} < \infty, \quad \text{for some } 0 \leq q < 1. \quad (12)$$

This result is very convenient since a vast literature concerning the covariance structure of dynamical systems is available. For instance, it is well known that if the dynamical system is hyperbolic, then the covariance decays exponentially fast (see Baladi, 2000; Hasselblatt and Katok, 1996) and the condition (12) holds for all $q \in [0, 1]$. Furthermore, if the system presents long range dependence in the sense that $\text{Cov}(\mu_t, \mu_{t+k}) \sim L(k)k^{-b}$, for $0 < b < 1$, for some slowly varying function L , then condition (12) holds, for all $1 - b < q < 1$. This is the case, for instance, for the Manneville-Pomeau map (Map 4) when $s \in (0.5, 1)$. Finally, in this context, (12) is a sufficient condition for a strong law of large number for Y_t to hold.

5 Partial Maximum Likelihood Inference

Parameter inference in the proposed can be done via partial maximum likelihood estimation (PMLE). Let $\{(y_t, \mathbf{x}'_t)\}_{t=1}^n$ be a sample from a β ARC(p) model following (2) and (3) for a given transformation $T_{\boldsymbol{\theta}}$ depending on an identifiable vector of parameters $\boldsymbol{\theta} = (\theta_1, \dots, \theta_r)' \in \Omega_T \subseteq \mathbb{R}^r$ and h a suitable link function. We shall assume that $u_0 \in (0, 1)$ is known and such that $T^t(u_0) \notin \{0, 1\}$ for all t . Let $\boldsymbol{\gamma} := (\nu, \alpha, \boldsymbol{\beta}', \boldsymbol{\phi}', \boldsymbol{\theta}')' \in \Omega \subseteq (0, \infty) \times \mathbb{R}^{p+l+1} \times \Omega_T$ be the $(l + p + r + 2)$ -dimensional vector of parameter related to the model, where Ω denotes the parameter space. Upon

writing

$$\begin{aligned}\ell_t(\boldsymbol{\gamma}) &= \log(f(y_t; \boldsymbol{\gamma} | \mathcal{F}_{t-1})) \\ &= \log(\Gamma(\nu)) - \log(\Gamma(\mu_t \nu)) - \log(\Gamma(\nu(1 - \mu_t))) + \\ &\quad + (\mu_t \nu - 1) \log(y_t) + (\nu(1 - \mu_t) - 1) \log(1 - y_t),\end{aligned}$$

the log-likelihood associated to model (2) and (3) is given by

$$\ell(\boldsymbol{\gamma}) := \sum_{t=1}^n \ell_t(\boldsymbol{\gamma}).$$

The partial maximum likelihood estimator is then define as

$$\hat{\boldsymbol{\gamma}} = \underset{\boldsymbol{\gamma} \in \Omega}{\operatorname{argmax}} \{\ell(\boldsymbol{\gamma})\}. \quad (13)$$

To obtain the PMLE we need to solve the optimization problem (13), which can be done upon finding the score function and solving a non-linear system, by using, for instance, the BFGS optimization algorithm. Alternatively, the optimization problem can also be solved by using other methods such as Nelder-Mead.

Since η_t is usually a non-linear function of $\boldsymbol{\theta}$, the asymptotic theory of the PMLE in the context of β ARC models requires some non-trivial adaptations of the exsiting theory for GARMA-like models (presented, for instance, in Fokianos and Kedem, 2004). This will be the subject of another paper. In the next section (and in the supplementary material accompanying the paper), we shall study the finite sample performance of the PMLE in the context of β ARC models, which, as we shall see, indicates that the PMLE is asymptotically normally distributed.

6 Monte Carlo Simulation

A Monte Carlo simulation study was performed to analise the finite sample performance of the pseudo-likelihood estimator on β ARC models considering two different type of maps: map 1 and map 3 (the logistic map). For map 1 we assume k fixed and known while for map 3 we assume both, θ fixed and unknown. Different values of ν were considered to generate models with small and large condicional variance. We also investigate the influence of k , θ and the sample size n . All codes were implemented in R (R Core Team, 2018) and are available upon request.

Data Generating Process

To generate the samples from the pure chaotic β ARC process the following was set.

- 1) For map 1 we consider $k \in \{3, 5, 7\}$ and for map 3 we consider $\theta \in \{1, 2, 3, 3.3, 3.6, 3.99\}$.
- 2) Three different values of ν were considered, namely, $\nu \in \{10, 40, 120\}$.
- 3) Three different values of u_0 were considered, namely, $u_0 \in \{0.2 + \pi/100, 0.5 + \pi/100, 0.8 + \pi/100\}$.
- 4) The time series $\{Y_t\}_{t=1}^n$ was generated as follows

$$\mu_t := T^{t-1}(u_0) \quad \text{and} \quad Y_t \sim \text{Beta}(\mu_t, \nu)$$

where T denotes map 1 or 3.

- 5) All time series were generated with sample size $n = 1000$.
- 6) For all scenarios we perform $re = 1000$ replications.

Parameter Estimation

To obtain the PMLE we solve the optimization problem (13). The following was set.

- 1) The maximization of the objective function was performed by considering the so-called Nelder-Mead algorithm implemented in the “lme4” package (Bates et al., 2015) in R (R Core Team, 2018).
- 2) In all scenarios, u_0 is assumed known.
- 3) To start the optimization algorithm we calculate the log-likelihood function in a grid of initial points and select as starting point the one with higher log-likelihood value.
- 4) The initial values for ν were $\{5, 50, 100\}$.
- 5) For map 3, when θ was assumed unknown, the initial values were $\{1.1, 2.1, 3.1, 3.5, 3.8\}$.
- 6) For all scenarios, estimation was performed by considering samples $\{Y_t\}_{t=1}^n$ with $n \in \{100, 500, 1000\}$ from the simulated time series.

Results

A supplementary material is provided accompanying this paper. The material contains all the tables and figures describing in details the simulation results. The study performed show that, as expected, as n increases, both, the estimator's bias and variance decrease so that the estimated values are close to the true ones. We found no relation between u_0 and the estimator's performance. As for the maps we observe the following.

- 1) For map 1, we found no relation between k and the estimation performance. The highest value (11.80%) for the mean absolute percentage error (MAPE) of estimation for ν was observed when $n = 100$, $k \in \{5, 7\}$ and $\nu = 120$. The lowest MAPE (3.04%) was observed when $n = 1000$, $k = 5$ and $\nu = 10$.
- 2) For map 3, assuming θ known, the estimated value of ν was always close to the true one. The highest MAPE (12.14%) for ν was observed when $n = 100$, $\theta = 2$ and $\nu = 120$. The lowest MAPE (2.54%) was observed when $n = 1000$, $\theta = 1.00$ and $\nu \in \{10, 40\}$.
- 3) For map 3, assuming θ unknown, when $\theta \in \{1, 2, 3, 3.3\}$ the estimated values of θ and ν are close to the true ones. The highest MAPE (16.76%) for the mean absolute percentage error (MAPE) of estimation for ν was observed when $n = 100$, $\theta = 1$ and $\nu = 10$. The lowest MAPE (3.42%) was observed when $n = 1000$, $\theta = 3.3$ and $\nu = 10$. For θ , the highest MAPE (2.39%) was observed when $n = 100$, $\theta = 2$ and $\nu = 10$. The the lowest MAPE (0.01%) was observed when $n = 1000$, $\theta \in \{1, 3\}$ and $\nu = 120$. When $\theta \in \{3.6, 3.99\}$ neither θ nor ν were correctly estimated. In view of this result, when θ is assumed unknown, we only report the results for $\theta < 3.6$.

The lack of satisfactory results when $\theta \geq 3.6$ is assumed unknown was not a surprise. It is well known in the literature of dynamical systems that for values of θ beyond 3.56995, the behavior of the usual orbits depends dramatically on the parameter θ , and even when θ vary in small intervals in (3.56995, 4) the map can exhibit very different behaviors, such as attracting periodic points of very different periods or the absence of attracting periodic points, when the map becomes a chaotic map. See Figure 7.

7 Conclusion

Here we introduced the Beta Autoregressive Chaotic (β ARC) processes, a class of dynamic models for time series taking values on the unit interval. The model follows similar structure of other GARMA-like models (in the sense of Benjamin et al., 2003).

The random component of the process was modeled through a beta distribution, conditioned on the past information, while the conditional mean was specified allowing the presence of covariates (random and/or deterministic) and an extra additive term defined by the iteration of a map T defined on $[0, 1]$, inspired on the theory of chaotic processes and dynamical systems. This additive term is able to model a wide variety of behaviors in the processes' conditional mean, including short and long range dependence, attracting and/or repelling fixed or periodic points, presence or absence of absolutely continuous invariant measure, among others, allowing for a much broader and flexible dependence structure compared to competitive GARMA-type models presented in the literature.

In the β ARC model, the extra additive term's definition borrows ideas from dynamical systems. For this reason, a review on the main definitions concerning one dimensional dynamical systems was presented in order to describe the wide variety of behaviors that T can present. Among the main features of the underlying transformation we focused on the existence of attracting and/or repelling fixed or periodic points and the presence or absence of absolutely continuous invariant measure. We also discussed how the characteristics of the chaotic process are reflected into the observed time series. In particular, we showed that, as the precision parameter ν increases, the closer the sample path resembles the conditional mean's dynamics. We also presented some examples where the systematic component can accommodate short or long range dependence, periodic behavior and/or laminar phases.

We also presented some theoretical results which are new in the literature in the sense that are not known for any other GARMA-like process. For instance, we derived the covariance structure of the β ARC models and obtained sufficient conditions for stationarity, law of large numbers and a Birkhoff-type result to hold. In particular, we showed that, in the absence of an autoregressive component, if T has an absolute continuous T -invariant measure and the covariate process is stationary, then the β ARC processes is stationary.

A Monte Carlo simulation study, considering maps 1 and 3 (the logistic map) was performed to assess the finite sample behavior of the partial maximum likelihood estimation procedure. The study showed that, as n increases, both the estimator's bias and variance decrease so that the estimated values are close to the true ones. No relation between u_0 and the estimator's performance was found. For the logistic map, assuming θ unknown lead to the lack of satisfactory results when the true parameter $\theta \geq 3.6$. This result was not a surprise given the well-known wild behavior of the logistic map for values of θ beyond 3.56995.

Acknowledgments

T.S. Prass gratefully acknowledges the support of FAPERGS (ARD 01/2017, Processo 17/2551-0000826-0).

References

- Baladi, V., 2000. Positive Transfer Operators and Decay of Correlations. World Scientific.
- Bates, D., Mächler, M., Bolker, B., Walker, S., 2015. Fitting linear mixed-effects models using lme4. *Journal of Statistical Software* 67 (1), 1–48.
- Bayer, F. M., Bayer, D. M., Pumi, G., 2017. Kumaraswamy autoregressive moving average models for double bounded environmental data. *Journal of Hydrology* 555, 385–396.
- Benjamin, M. A., Rigby, R. A., Stasinopoulos, D. M., 2003. Generalized autoregressive moving average models. *Journal of the American Statistical Association* 98 (461), 214–223.
- Box, G., Jenkins, G. M., Reinsel, G., 2008. Time series analysis: forecasting and control. Hardcover, John Wiley & Sons.
- Boyarsky, A., Gora, P., 1997. Laws of Chaos. Birkhauser.
- Brockwell, P. J., Davis, R. A., 1991. Time Series: Theory and Methods, 2nd Edition. Springer-Verlag.
- de Melo, W., Van Strien, S., 1993. One-Dimensional Dynamics. Springer-Verlag.
- Devaney, R. L., 2003. An Introduction to Chaotic Dynamical Systems, 2nd Edition. CRC Press.
- Ding, J., Zhou, A., 2009. Statistical properties of deterministic systems. Springer Science & Business Media.
- Eckmann, J. P., 1981. Roads to turbulence in dissipative dynamical systems. *Rev. Mod. Phys.* 53, 643–654.
- Ferrari, S. L. P., Cribari-Neto, F., 2004. Beta regression for modelling rates and proportions. *Journal of Applied Statistics* 31 (7), 799–815.
- Fokianos, K., Kedem, B., 2004. Partial likelihood inference for time series following generalized linear models. *Journal of Time Series Analysis* 25 (2), 173–197.
- Hasselblatt, B., Katok, A., 1996. Introduction to the Modern Theory of Dynamical Systems. Cambridge University Press.

- Honsking, J. R. M., 1981. Fractional differencing. *Biometrika* 1 (68), 165–176.
- Hu, T.-C., Rosalsky, A., Volodin, A., 2008. On convergence properties of sums of dependent random variables under second moment and covariance restrictions. *Statistics & Probability Letters* 78 (14), 1999 – 2005.
- Lasota, A., Yorke, J. A., 1973. On the existence of invariant measures for piecewise monotonic transformations. *Transactions of the American Mathematical Society* 186, 481–488.
- Lopes, A., Lopes, S., Souza, R. R., 1996. Spectral analysis of chaotic transformations. *Brazilian Journal of Probability and Statistics* 10 (2), 151–179.
- Palma, W., 2007. Long-Memory Time Series: Theory and Methods. Wiley Series in Probability and Statistics. Wiley.
- Pumi, G., Valk, M., Bisognin, C., Bayer, F. M., Prass, T. S., 2019. Beta autoregressive fractionally integrated moving average models. *Journal of Statistical Planning and Inference* 200, 196–212.
- R Core Team, 2018. R: A Language and Environment for Statistical Computing. R Foundation for Statistical Computing, Vienna, Austria.
URL <https://www.R-project.org/>
- Robinson, C., 1998. Dynamical Systems: Stability, Symbolic Dynamics, and Chaos, 2nd Edition. CRC Press.
- Rocha, A. V., Cribari-Neto, F., 2009. Beta autoregressive moving average models. *Test* 18 (3), 529–545.
- Thaler, M., 1980. Estimates of the invariant densities of endomorphisms with indifferent fixed points. *Israel Journal of Mathematics* 37 (4), 303–314.
- Walters, P., 1982. An Introduction to Ergodic Theory. Springer-Verlag.
- Zebrowsky, J. J., 2001. Intermittency in human heart rate variability. *Acta Physica Polonica B* 32, 1531–1540.
- Zeger, S. L., Qaqish, B., 1988. Markov regression models for time series: a quasi-likelihood approach. *Biometrics* 44 (4), 1019–1031.

A Dynamic Model for Double Bounded Time Series With Chaotic Driven Conditional Averages - Supplementary Material

February 1, 2019

This is a supplementary material for the paper *A Dynamic Model for Double Bounded Time Series With Chaotic Driven Conditional Averages*. Here we present figures and tables describing in details the simulation results.

1 Monte Carlo Simulation

A Monte Carlo simulation study was performed to analyse the finite sample performance of the pseudo-likelihood estimator on β ARC models considering two different type of maps: map 1 and map 3 (the logistic map). For map 1 we assume k fixed and known while for map 3 we assume both, θ fixed and unknown. Different values of ν were considered to generate models with small and large conditional variance. We also investigate the influence of k , θ and the sample size n . All codes were implemented in R and are available upon request.

Data Generating Process

To generate the samples from the pure chaotic β ARC process the following was set.

- 1) For map 1 we consider $k \in \{3, 5, 7\}$ and for map 3 we consider $\theta \in \{1, 2, 3, 3.3, 3.6, 3.99\}$.
- 2) Three different values of ν were considered, namely, $\nu \in \{10, 40, 120\}$.
- 3) Three different values of u_0 were considered, namely, $u_0 \in \{0.2 + \pi/100, 0.5 + \pi/100, 0.8 + \pi/100\}$.
- 4) The time series $\{Y_t\}_{t=1}^n$ was generated as follows

$$\mu_t := T^{t-1}(u_0) \quad \text{and} \quad Y_t \sim \text{Beta}(\mu_t, \nu)$$

were T denotes map 1 or 3.

- 5) All time series were generated with sample size $n = 1,000$.
- 6) For all scenarios we perform $re = 1,000$ replications.

Parameter Estimation

To obtain the PMLE we solve the optimization problem

$$\hat{\gamma} = \operatorname{argmax}_{\gamma \in \Omega} \{\ell(\gamma)\}.$$

The following was set.

- 1) The maximization of the objective function was performed by considering the so-called Nelder-Mead algorithm implemented in the “lme4” package in R.
- 2) In all scenarios, u_0 is assumed known.
- 3) To start the optimization algorithm we calculate the log-likelihood function in a grid of initial points and select as starting point the one with higher log-likelihood value.
- 4) The initial values for ν were $\{5, 50, 100\}$.
- 5) For map 3, when θ was assumed unknown, the initial values were $\{1.1, 2.1, 3.1, 3.5, 3.8\}$.
- 6) For all scenarios, estimation was performed by considering samples $\{Y_t\}_{t=1}^n$ with $n \in \{100, 500, 1000\}$ from the simulated time series.

1.1 Simulation Results

The study performed show that, as expected, as n increases, both, the estimator’s bias and variance decrease so that the estimated values are close to the true ones. We found no relation between u_0 and the estimator’s performance. As for the maps we observe the following (the worst and best results are highlighted in the mentioned tables, in red and blue, respectively).

- 1) For map 1, we found no relation between k and the estimation performance. The highest value (11.80%) for the mean absolute percentage error (MAPE) of estimation for ν was observed when $n = 100$, $k \in \{5, 7\}$ and $\nu = 120$. The lowest MAPE (3.04%) was observed when $n = 1000$, $k = 5$ and $\nu = 10$.
- 2) For map 3, assuming θ known, the estimated value of ν was always close to the true one. The highest MAPE (12.14%) for ν was observed when $n = 100$, $\theta = 2$ and $\nu = 120$. The lowest MAPE (2.54%) was observed when $n = 1000$, $\theta = 1.00$ and $\nu \in \{10, 40\}$.
- 3) For map 3, assuming θ unknown, when $\theta \in \{1, 2, 3, 3.3\}$ the estimated values of θ and ν are close to the true ones. The highest MAPE (16.76%) for the mean absolute percentage error (MAPE) of estimation for ν was observed when $n = 100$, $\theta = 1$ and $\nu = 10$. The lowest MAPE (3.42%) was observed when $n = 1000$, $\theta = 3.3$ and $\nu = 10$. For θ , the highest MAPE (2.39%) was observed when $n = 100$, $\theta = 2$ and $\nu = 10$. The lowest MAPE (0.01%) was observed when $n = 1000$, $\theta \in \{1, 3\}$ and $\nu = 120$. When $\theta \in \{3.6, 3.99\}$ neither θ nor ν were correctly estimated. In view of this result, when θ is assumed unknown, we only report the results for $\theta < 3.6$.

The lack of satisfactory results when $\theta \geq 3.6$ is assumed unknown was not a surprise. It is well known in the literature of dynamical systems that for values of θ beyond 3.56995, the behavior of the usual orbits depends dramatically on the parameter θ , and even when θ vary in small intervals in $(3.56995, 4)$ the map can exhibit very different behaviors, such as attracting periodic points of very different periods or the absence of attracting periodic points, when the map becomes a chaotic map.

Simulation Results for Map 1

Table 1: Simulation Results for parameter ν considering Map 1 with $k \in \{3, 5, 7\}$ and sample size $n \in \{100, 500, 1000\}$: the mean estimated value of ν over 1,000 replications ($\bar{\nu}$), for $\nu \in \{10, 40, 120\}$, the standard deviation of the estimates (sd_ν) and the mean absolute percentage error (MAPE).

k	u_0	$n = 100$			$n = 500$			$n = 1,000$		
		$\bar{\nu}$	sd_ν	MAPE	$\bar{\nu}$	sd_ν	MAPE	$\bar{\nu}$	sd_ν	MAPE
$\nu = 10$										
3	$0.2 + \frac{\pi}{100}$	10.32	1.3381	10.57	10.04	0.5515	4.39	10.04	0.4113	3.25
	$0.5 + \frac{\pi}{100}$	10.25	1.3845	10.84	10.18	0.5868	4.84	10.17	0.4252	3.62
	$0.8 + \frac{\pi}{100}$	10.31	1.4106	11.13	10.11	0.6056	4.89	10.06	0.4094	3.25
5	$0.2 + \frac{\pi}{100}$	10.19	1.3591	10.72	10.03	0.5703	4.57	10.05	0.3848	3.04
	$0.5 + \frac{\pi}{100}$	10.21	1.3493	10.56	10.08	0.5855	4.70	10.09	0.4014	3.24
	$0.8 + \frac{\pi}{100}$	10.25	1.3489	10.61	10.15	0.5864	4.79	10.06	0.4100	3.29
7	$0.2 + \frac{\pi}{100}$	10.17	1.3458	10.51	10.13	0.6009	4.85	10.07	0.4033	3.28
	$0.5 + \frac{\pi}{100}$	10.47	1.3961	11.34	10.11	0.5827	4.72	10.09	0.4183	3.39
	$0.8 + \frac{\pi}{100}$	10.33	1.2762	10.23	10.07	0.5692	4.57	10.07	0.4182	3.32
$\nu = 40$										
3	$0.2 + \frac{\pi}{100}$	40.82	5.6650	11.10	40.12	2.4435	4.86	40.10	1.7364	3.49
	$0.5 + \frac{\pi}{100}$	40.60	5.5280	10.75	40.54	2.5651	5.22	40.50	1.7968	3.63
	$0.8 + \frac{\pi}{100}$	40.83	5.7697	11.19	40.11	2.5445	5.03	40.23	1.7728	3.55
5	$0.2 + \frac{\pi}{100}$	40.85	5.6999	11.29	40.23	2.4453	4.87	40.15	1.6681	3.31
	$0.5 + \frac{\pi}{100}$	40.96	5.9714	11.74	40.10	2.4866	4.92	40.28	1.7743	3.55
	$0.8 + \frac{\pi}{100}$	40.61	5.7288	11.05	40.13	2.4419	4.86	40.15	1.7566	3.48
7	$0.2 + \frac{\pi}{100}$	40.77	5.7992	11.18	40.33	2.4422	4.91	40.14	1.8068	3.68
	$0.5 + \frac{\pi}{100}$	41.06	5.6579	11.07	40.19	2.5291	5.02	40.17	1.7392	3.45
	$0.8 + \frac{\pi}{100}$	40.57	5.7672	11.22	40.15	2.4404	4.88	40.11	1.7784	3.50
$\nu = 120$										
3	$0.2 + \frac{\pi}{100}$	122.91	17.5366	11.49	120.65	7.8294	5.16	120.28	5.4909	3.68
	$0.5 + \frac{\pi}{100}$	122.52	16.5041	10.82	121.53	7.5306	5.13	120.82	5.3160	3.57
	$0.8 + \frac{\pi}{100}$	123.23	17.6172	11.31	120.31	7.7391	5.10	120.32	5.1570	3.42
5	$0.2 + \frac{\pi}{100}$	122.29	17.0783	11.29	120.19	7.7037	5.15	120.15	5.3979	3.54
	$0.5 + \frac{\pi}{100}$	123.37	17.9182	11.80	120.42	7.5763	4.97	120.27	5.1632	3.37
	$0.8 + \frac{\pi}{100}$	122.32	17.4805	11.50	120.37	7.4695	4.98	120.27	5.3142	3.50
7	$0.2 + \frac{\pi}{100}$	122.89	17.8409	11.77	121.10	7.3435	4.92	120.60	5.2435	3.51
	$0.5 + \frac{\pi}{100}$	122.16	17.7107	11.59	120.73	7.6709	4.99	120.53	5.3640	3.58
	$0.8 + \frac{\pi}{100}$	122.30	18.2375	11.80	120.76	7.8141	5.19	120.24	5.2169	3.46

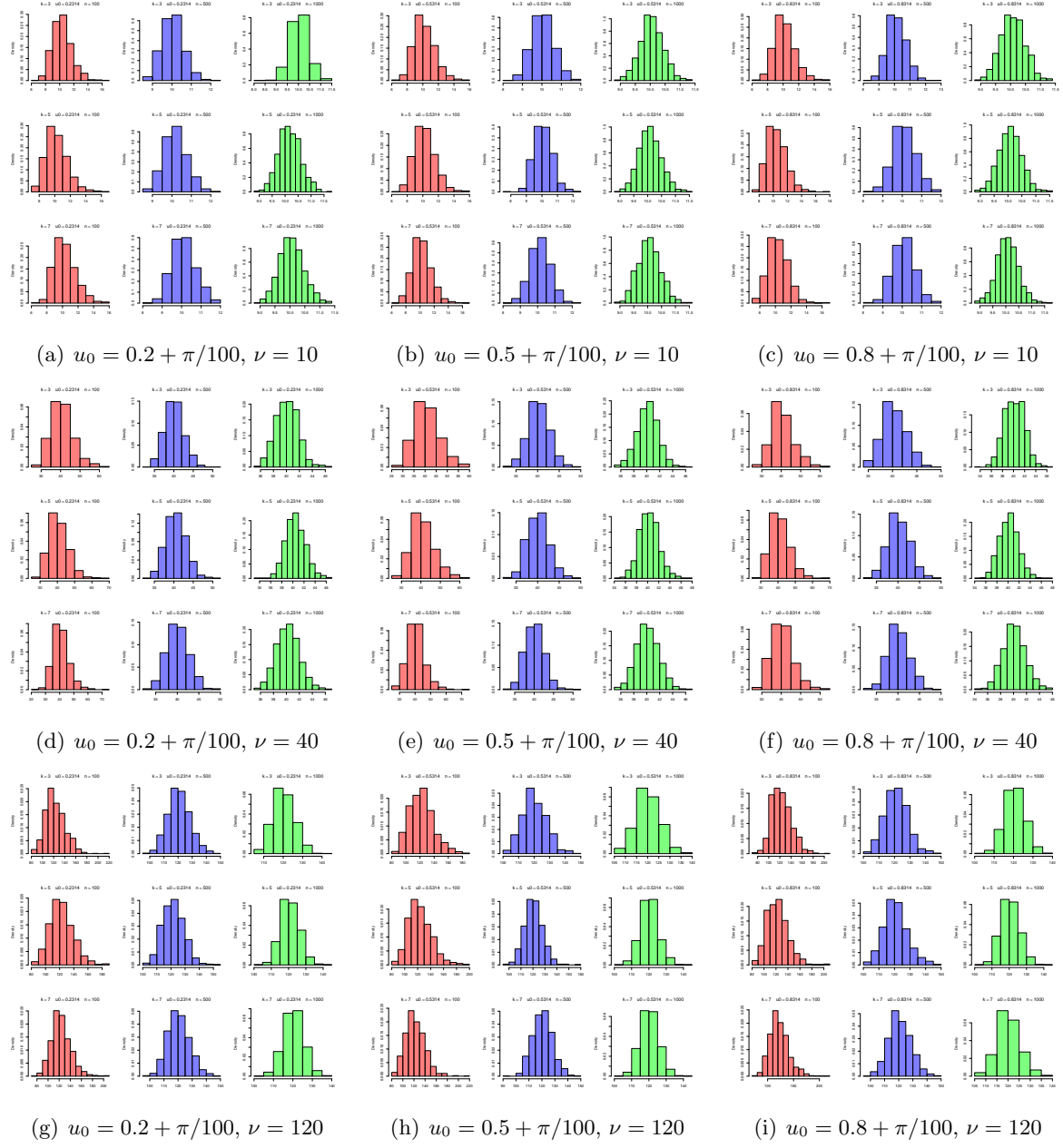


Figure 1: Histogram considering the estimated values, from 1,000 replications, for the parameter ν considering Map 1 with $k \in \{3, 5, 7\}$ (first, second and third row of each subfigure, respectively), when $n \in \{100, 500, 1000\}$ (red, blue and green, respectively).

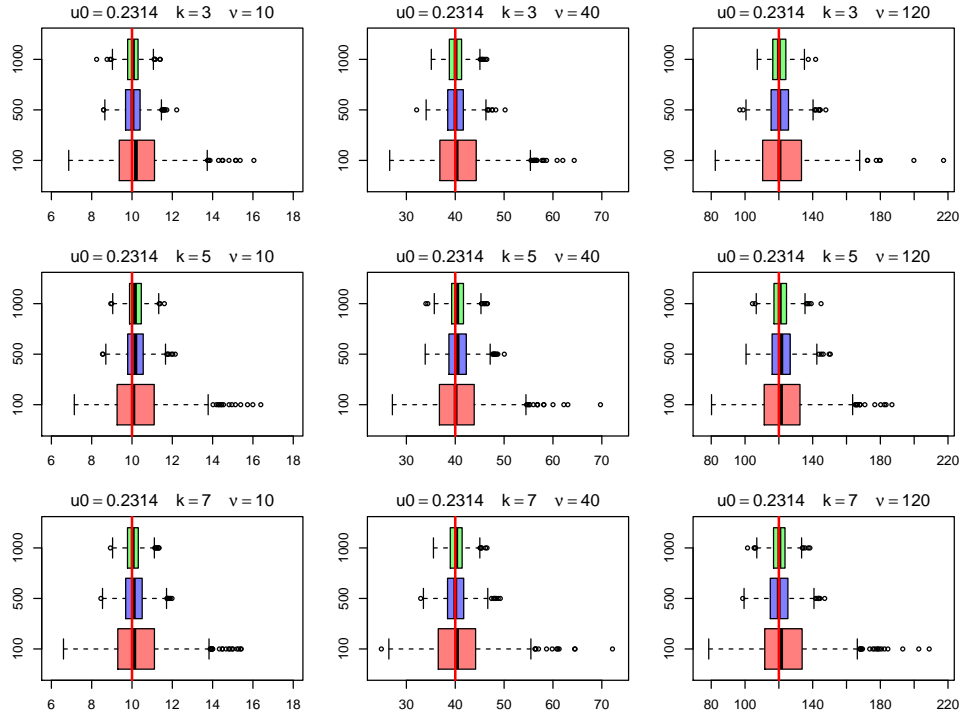


Figure 2: Box-plot considering the estimated values, from 1,000 replications, for the parameter $\nu \in \{10, 40, 120\}$ (from left to right), considering Map 1 with $k \in \{3, 5, 7\}$ (from top to bottom) and $u_0 = 0.2 + \pi/100$.

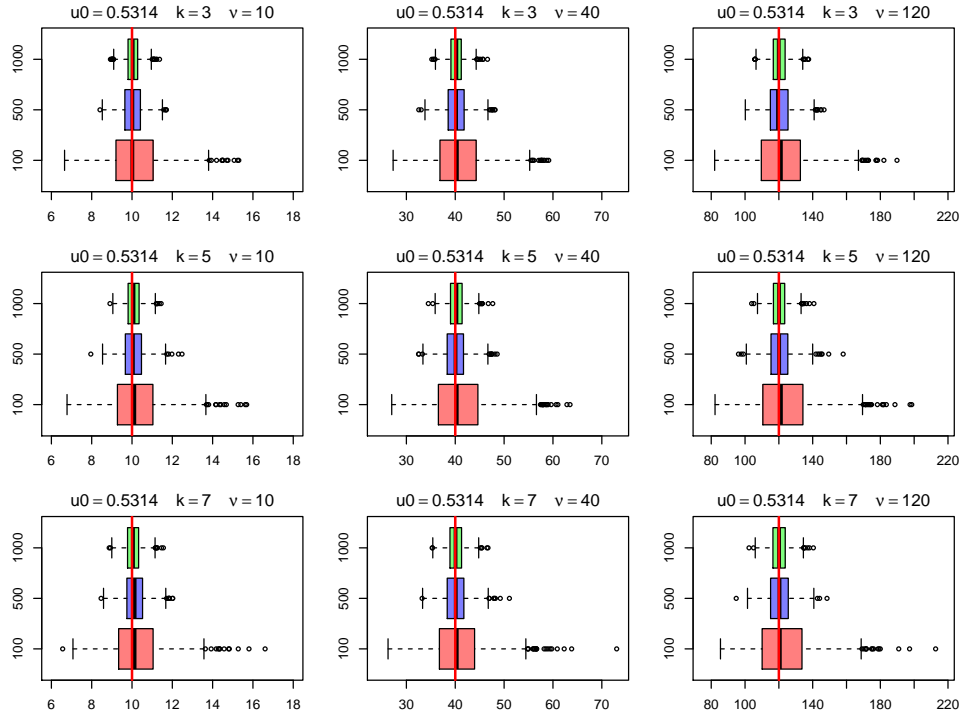


Figure 3: Box-plot considering the estimated values, from 1,000 replications, for the parameter $\nu \in \{10, 40, 120\}$ (from left to right), considering Map 1 with $k \in \{3, 5, 7\}$ (from top to bottom) and $u_0 = 0.5 + \pi/100$.

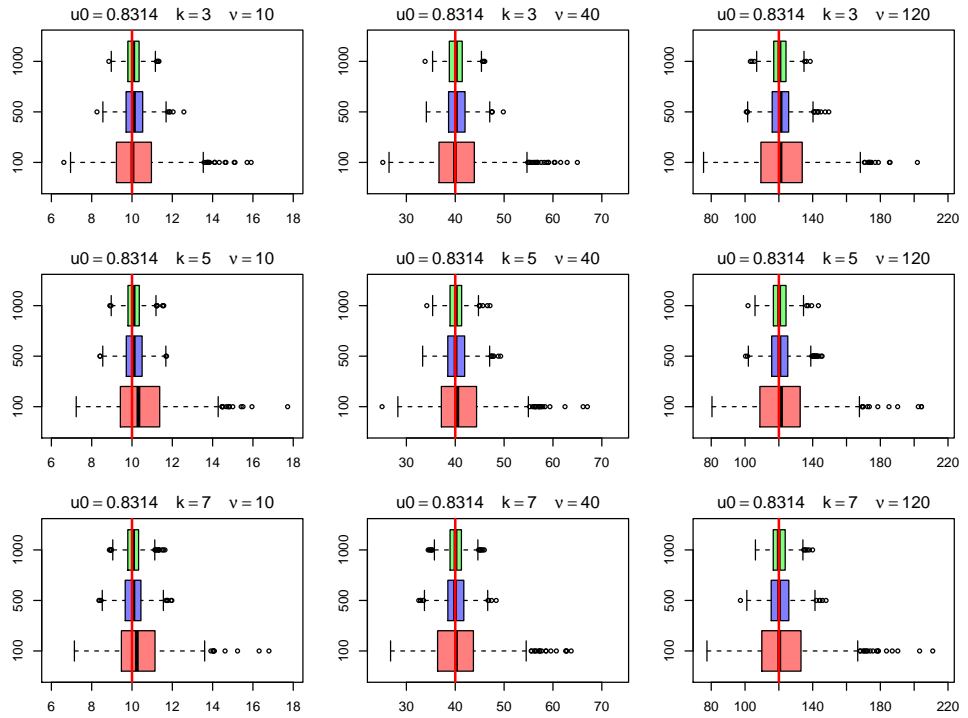


Figure 4: Box-plot considering the estimated values, from 1,000 replications, for the parameter $\nu \in \{10, 40, 120\}$ (from left to right), considering Map 1 with $k \in \{3, 5, 7\}$ (from top to bottom) and $u_0 = 0.8 + \pi/100$.

Simulation Results for Map 3

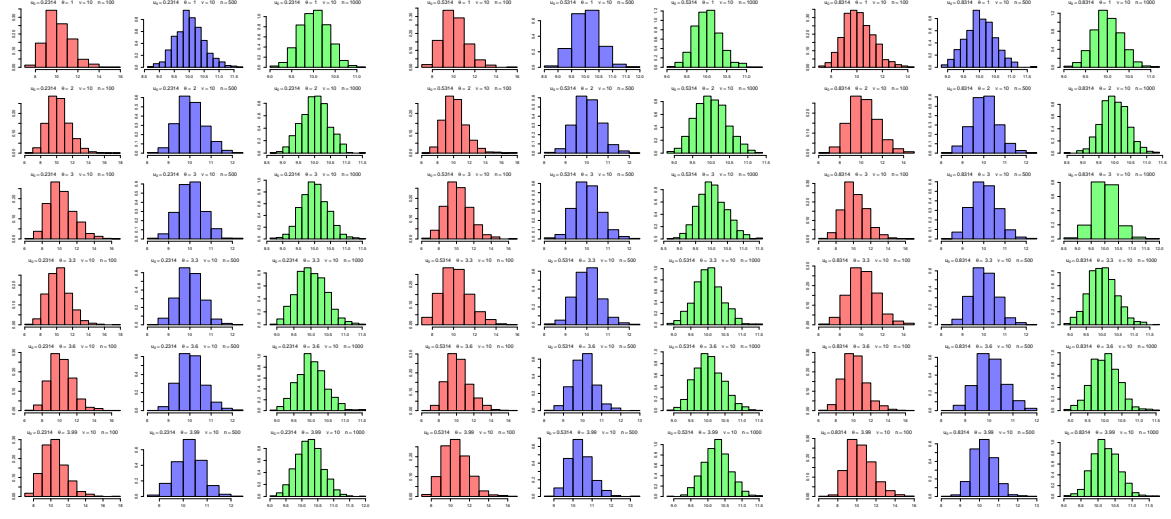
Table 2: Simulation Results for parameter ν considering Map 3, with θ assumed known, and sample size $n \in \{100, 500, 1000\}$: the mean estimated value of ν over 1,000 replications ($\bar{\nu}$), for $\nu \in \{10, 40, 120\}$, the standard deviation of the estimates (sd_ν) and the mean absolute percentage error (MAPE).

k	u_0	$n = 100$			$n = 500$			$n = 1,000$		
		$\bar{\nu}$	sd_ν	MAPE	$\bar{\nu}$	sd_ν	MAPE	$\bar{\nu}$	sd_ν	MAPE
$\nu = 10$										
1.0	$0.2 + \frac{\pi}{100}$	10.15	1.1801	9.32	10.02	0.4710	3.70	10.02	0.3279	2.64
	$0.5 + \frac{\pi}{100}$	10.06	1.1335	8.88	10.03	0.4741	3.80	10.01	0.3255	2.56
	$0.8 + \frac{\pi}{100}$	10.13	1.1379	9.07	10.02	0.4583	3.67	10.00	0.3206	2.54
2.0	$0.2 + \frac{\pi}{100}$	10.24	1.3850	10.85	10.05	0.6271	5.02	10.01	0.4213	3.38
	$0.5 + \frac{\pi}{100}$	10.19	1.4351	10.99	10.04	0.5853	4.63	10.00	0.4259	3.45
	$0.8 + \frac{\pi}{100}$	10.20	1.3396	10.69	10.06	0.6046	4.81	9.98	0.4117	3.29
3.0	$0.2 + \frac{\pi}{100}$	10.20	1.4895	11.63	10.05	0.5967	4.77	9.99	0.4174	3.33
	$0.5 + \frac{\pi}{100}$	10.16	1.4230	11.23	10.03	0.6159	4.88	10.02	0.4397	3.49
	$0.8 + \frac{\pi}{100}$	10.16	1.3869	11.00	10.04	0.6064	4.87	10.00	0.4252	3.34
3.3	$0.2 + \frac{\pi}{100}$	10.26	1.3851	10.86	9.99	0.5792	4.60	10.01	0.4296	3.46
	$0.5 + \frac{\pi}{100}$	10.17	1.3480	10.72	10.04	0.6015	4.72	10.02	0.4125	3.25
	$0.8 + \frac{\pi}{100}$	10.14	1.3344	10.51	10.01	0.5894	4.71	10.02	0.4336	3.46
3.6	$0.2 + \frac{\pi}{100}$	10.19	1.3602	10.72	10.05	0.5897	4.65	10.01	0.4180	3.28
	$0.5 + \frac{\pi}{100}$	10.21	1.3649	10.65	10.06	0.5890	4.60	10.03	0.4194	3.35
	$0.8 + \frac{\pi}{100}$	10.16	1.3208	10.18	10.05	0.5979	4.73	10.00	0.4054	3.21
3.99	$0.2 + \frac{\pi}{100}$	10.40	1.3551	10.71	10.25	0.5609	4.86	10.24	0.4036	3.73
	$0.5 + \frac{\pi}{100}$	10.58	1.3403	11.33	10.37	0.5904	5.37	10.26	0.3815	3.72
	$0.8 + \frac{\pi}{100}$	10.36	1.3274	10.51	10.23	0.5745	4.86	10.22	0.3856	3.49
$\nu = 40$										
1.0	$0.2 + \frac{\pi}{100}$	40.78	5.1616	10.28	40.01	1.9683	3.89	40.09	1.2942	2.57
	$0.5 + \frac{\pi}{100}$	40.79	4.9338	9.72	40.24	1.9540	3.91	40.03	1.2744	2.54
	$0.8 + \frac{\pi}{100}$	40.52	5.3058	10.24	40.12	1.9830	3.98	40.09	1.3250	2.66
2.0	$0.2 + \frac{\pi}{100}$	40.86	5.8204	11.33	40.32	2.4512	4.88	40.09	1.7758	3.53
	$0.5 + \frac{\pi}{100}$	40.89	5.9390	11.68	40.23	2.5005	4.99	40.03	1.7559	3.46
	$0.8 + \frac{\pi}{100}$	40.59	5.7425	11.20	40.22	2.5336	5.09	40.04	1.7577	3.50
3.0	$0.2 + \frac{\pi}{100}$	40.90	5.8181	11.29	40.07	2.4581	4.87	40.05	1.7317	3.47
	$0.5 + \frac{\pi}{100}$	41.10	5.9425	11.82	39.97	2.5282	5.05	40.09	1.8172	3.60
	$0.8 + \frac{\pi}{100}$	41.04	5.9787	11.82	40.14	2.6239	5.18	40.12	1.7550	3.52
3.3	$0.2 + \frac{\pi}{100}$	41.15	5.7604	11.28	40.12	2.5799	5.25	40.03	1.8055	3.59
	$0.5 + \frac{\pi}{100}$	41.18	5.8735	11.63	40.07	2.4675	4.93	40.10	1.7372	3.50
	$0.8 + \frac{\pi}{100}$	40.89	5.6721	11.35	40.16	2.4468	4.83	40.12	1.7495	3.47

(continues on the next page)

Table 3: Simulation Results for parameter ν considering Map 3, with θ assumed known, and sample size $n \in \{100, 500, 1000\}$: the mean estimated value of ν over 1,000 replications ($\bar{\nu}$), for $\nu \in \{10, 40, 120\}$, the standard deviation of the estimates (sd_{ν}) and the mean absolute percentage error (MAPE). **(continuing)**

k	u_0	$n = 100$			$n = 500$			$n = 1,000$		
		$\bar{\nu}$	sd_{ν}	MAPE	$\bar{\nu}$	sd_{ν}	MAPE	$\bar{\nu}$	sd_{ν}	MAPE
$\nu = 40$										
3.6	$0.2 + \frac{\pi}{100}$	40.72	5.7931	11.21	40.08	2.4043	4.80	40.03	1.7428	3.47
	$0.5 + \frac{\pi}{100}$	41.12	5.9605	11.80	40.19	2.4442	4.89	40.09	1.7357	3.45
	$0.8 + \frac{\pi}{100}$	40.77	5.8026	11.40	40.07	2.4937	4.92	40.16	1.7841	3.55
3.99	$0.2 + \frac{\pi}{100}$	40.87	5.6466	11.04	40.25	2.3722	4.72	40.16	1.6469	3.29
	$0.5 + \frac{\pi}{100}$	41.11	5.5884	10.90	40.29	2.4035	4.78	40.16	1.6665	3.37
	$0.8 + \frac{\pi}{100}$	40.81	5.3526	10.74	40.09	2.3401	4.72	40.12	1.6020	3.14
$\nu = 120$										
1.0	$0.2 + \frac{\pi}{100}$	122.77	16.4400	10.98	120.48	6.4470	4.28	120.07	4.2110	2.79
	$0.5 + \frac{\pi}{100}$	122.10	16.7165	10.81	120.45	6.1882	4.09	119.90	4.3003	2.85
	$0.8 + \frac{\pi}{100}$	122.44	16.8686	11.12	120.33	6.4084	4.19	120.29	4.3866	2.90
2.0	$0.2 + \frac{\pi}{100}$	122.81	18.1256	12.14	120.59	7.8174	5.22	120.28	5.2505	3.47
	$0.5 + \frac{\pi}{100}$	123.28	17.6939	11.51	120.75	7.8185	5.18	120.32	5.3456	3.50
	$0.8 + \frac{\pi}{100}$	123.01	17.0421	11.29	120.10	7.8189	5.19	120.54	5.3446	3.61
3.0	$0.2 + \frac{\pi}{100}$	122.64	17.6313	11.59	120.06	7.5920	5.08	120.29	5.3034	3.53
	$0.5 + \frac{\pi}{100}$	123.21	18.3460	11.99	120.56	7.4425	4.91	119.97	5.2674	3.47
	$0.8 + \frac{\pi}{100}$	122.07	17.2228	11.41	120.59	7.5574	4.99	120.49	5.3194	3.53
3.3	$0.2 + \frac{\pi}{100}$	122.95	18.2195	11.85	120.88	7.6848	5.17	120.55	5.2998	3.55
	$0.5 + \frac{\pi}{100}$	121.79	16.7350	11.11	119.90	7.7230	5.18	120.02	5.3366	3.56
	$0.8 + \frac{\pi}{100}$	122.71	17.2415	11.35	120.26	7.3743	4.90	119.99	5.4408	3.61
3.6	$0.2 + \frac{\pi}{100}$	122.19	17.7310	11.74	120.82	7.5467	5.03	120.32	5.3501	3.57
	$0.5 + \frac{\pi}{100}$	122.28	17.8908	11.52	120.52	7.3564	4.84	120.33	5.4521	3.62
	$0.8 + \frac{\pi}{100}$	122.21	17.5376	11.54	120.25	7.6120	5.09	120.34	5.2275	3.48
3.99	$0.2 + \frac{\pi}{100}$	122.02	16.0921	10.76	120.99	7.5722	5.01	120.15	5.2488	3.52
	$0.5 + \frac{\pi}{100}$	122.01	17.0835	11.27	120.37	7.6983	5.13	120.26	5.2090	3.51
	$0.8 + \frac{\pi}{100}$	122.16	16.8202	11.06	120.11	7.2527	4.75	120.18	5.4034	3.62



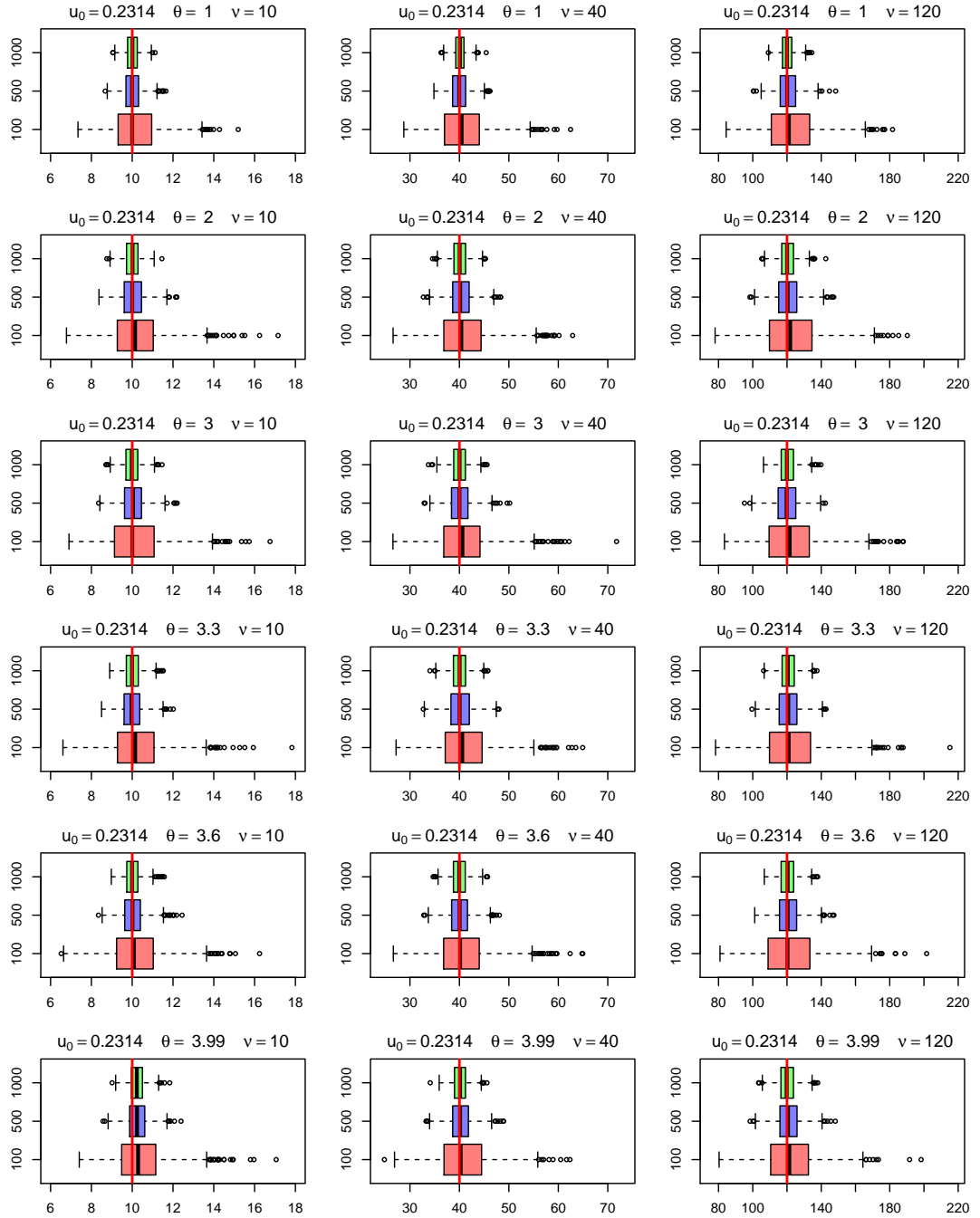


Figure 6: Simulation Results for the parameter $\nu \in \{10, 40, 120\}$ (from left to right) considering the Logistic Map with $u_0 = 0.2 + \pi/100$, when $n \in \{100, 500, 1000\}$ and $\theta \in \{1, 2, 3, 3.3, 3.6, 3.99\}$ (from top to bottom) is assumed known.

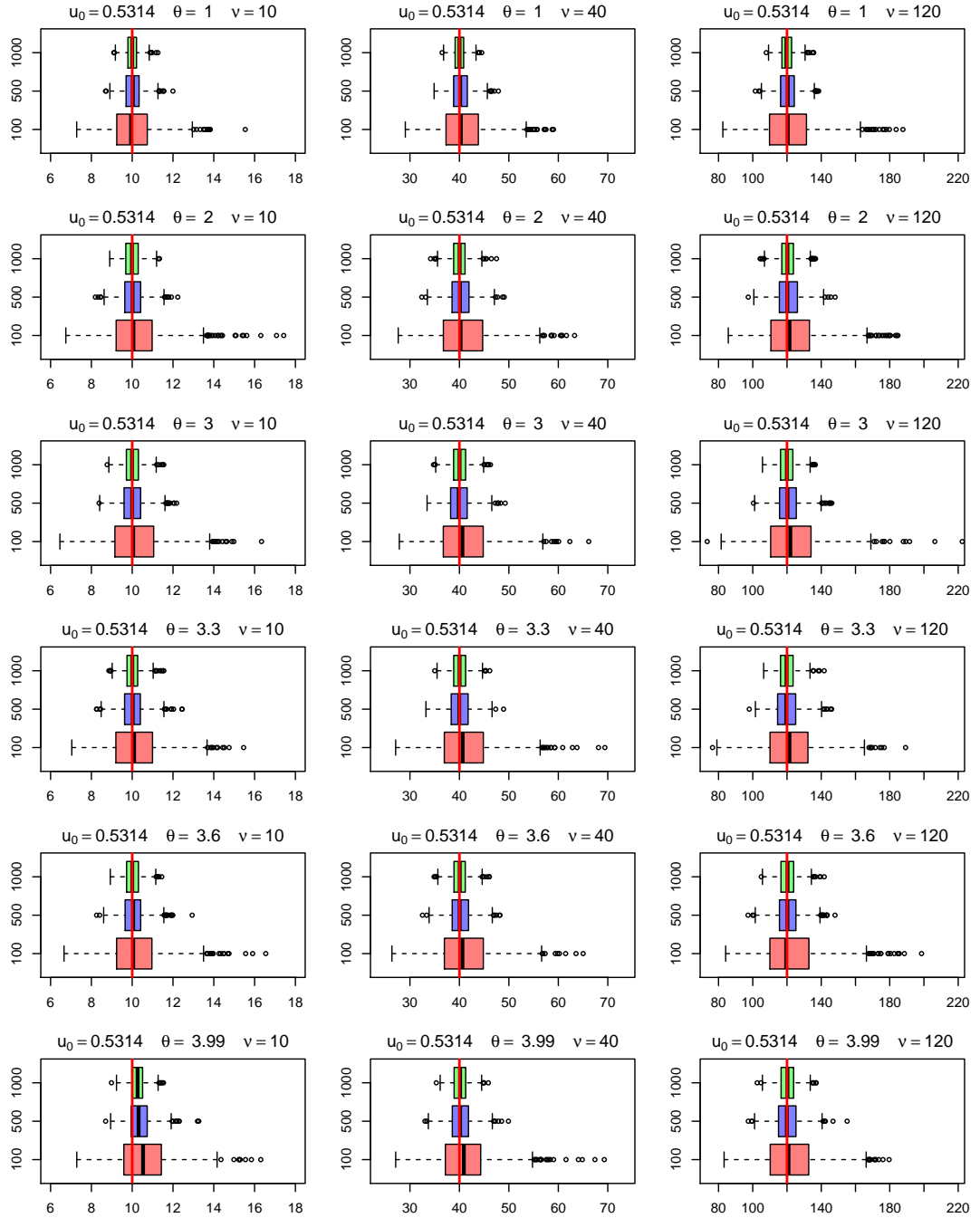


Figure 7: Simulation Results for the parameter $\nu \in \{10, 40, 120\}$ (from left to right) considering the Logistic Map with $u_0 = 0.5 + \pi/100$, when $n \in \{100, 500, 1000\}$ and $\theta \in \{1, 2, 3, 3.3, 3.6, 3.99\}$ (from top to bottom) is assumed known.

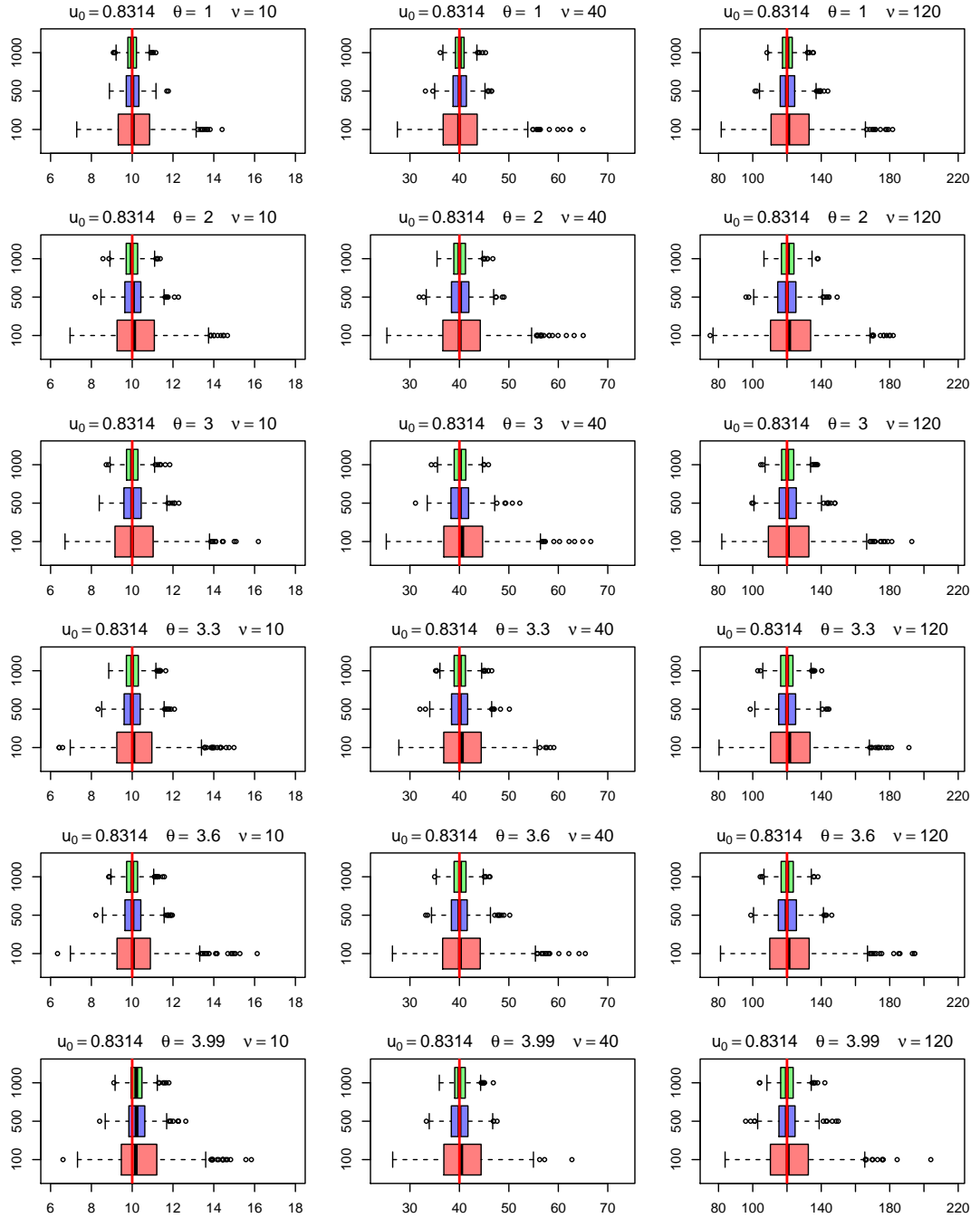


Figure 8: Simulation Results for the parameter $\nu \in \{10, 40, 120\}$ (from left to right) considering the Logistic Map with $u_0 = 0.8 + \pi/100$, when $n \in \{100, 500, 1000\}$ and $\theta \in \{1, 2, 3, 3.3, 3.6, 3.99\}$ (from top to bottom) is assumed known.

Table 4: Simulation Results for parameter ν considering Map 3, with θ assumed unknown, and sample size $n \in \{100, 500, 1000\}$: the mean estimated value of ν over 1,000 replications ($\bar{\nu}$), for $\nu \in \{10, 40, 120\}$, the standard deviation of the estimates (sd_{ν}) and the mean absolute percentage error (MAPE).

k	u_0	$n = 100$			$n = 500$			$n = 1,000$		
		$\bar{\nu}$	sd_{ν}	MAPE	$\bar{\nu}$	sd_{ν}	MAPE	$\bar{\nu}$	sd_{ν}	MAPE
$\nu = 10$										
1.0	$0.2 + \frac{\pi}{100}$	10.53	2.0516	16.22	10.09	0.9501	7.56	10.05	0.6466	5.23
	$0.5 + \frac{\pi}{100}$	10.43	2.0774	16.23	10.03	0.9288	7.44	10.05	0.6727	5.41
	$0.8 + \frac{\pi}{100}$	10.40	2.1660	16.76	10.10	0.9394	7.44	10.03	0.6437	5.09
2.0	$0.2 + \frac{\pi}{100}$	10.27	1.3836	10.84	10.07	0.6001	4.69	10.04	0.4297	3.48
	$0.5 + \frac{\pi}{100}$	10.25	1.3616	10.65	10.06	0.6123	4.87	10.03	0.4267	3.43
	$0.8 + \frac{\pi}{100}$	10.28	1.4245	11.19	10.09	0.6159	4.96	10.04	0.4317	3.44
3.0	$0.2 + \frac{\pi}{100}$	10.34	1.4818	11.78	10.03	0.5992	4.76	10.04	0.4234	3.43
	$0.5 + \frac{\pi}{100}$	10.31	1.4805	11.61	10.05	0.6228	5.01	10.02	0.4369	3.43
	$0.8 + \frac{\pi}{100}$	10.20	1.4192	11.23	10.07	0.6094	4.90	10.03	0.4426	3.57
3.3	$0.2 + \frac{\pi}{100}$	10.41	1.5193	12.04	10.06	0.6043	4.78	10.02	0.4328	3.44
	$0.5 + \frac{\pi}{100}$	10.33	1.4278	11.30	10.07	0.6086	4.90	10.03	0.4278	3.42
	$0.8 + \frac{\pi}{100}$	10.36	1.3631	10.79	10.06	0.6269	4.96	10.05	0.4396	3.54
$\nu = 40$										
1.0	$0.2 + \frac{\pi}{100}$	41.25	6.8677	13.65	40.28	3.5787	7.06	40.21	2.5430	5.15
	$0.5 + \frac{\pi}{100}$	41.60	6.8749	13.45	40.28	3.5664	7.04	40.03	2.5738	5.08
	$0.8 + \frac{\pi}{100}$	41.44	7.1384	13.85	40.26	3.6077	7.12	40.10	2.6340	5.26
2.0	$0.2 + \frac{\pi}{100}$	41.21	6.0024	11.91	40.36	2.5289	4.99	40.13	1.8560	3.69
	$0.5 + \frac{\pi}{100}$	41.29	6.0610	11.89	40.33	2.5671	5.15	40.22	1.7950	3.58
	$0.8 + \frac{\pi}{100}$	41.45	5.9185	11.75	40.21	2.6049	5.20	40.04	1.8396	3.67
3.0	$0.2 + \frac{\pi}{100}$	40.92	5.7206	11.31	40.25	2.5459	5.13	40.07	1.7913	3.59
	$0.5 + \frac{\pi}{100}$	41.37	5.8992	11.71	40.34	2.5380	5.06	40.06	1.7180	3.48
	$0.8 + \frac{\pi}{100}$	41.19	6.0721	11.81	40.40	2.5208	5.15	40.17	1.7317	3.43
3.3	$0.2 + \frac{\pi}{100}$	41.36	5.8271	11.80	40.24	2.5201	5.12	40.12	1.8301	3.63
	$0.5 + \frac{\pi}{100}$	41.22	6.1191	11.94	40.16	2.5315	5.11	40.16	1.7972	3.61
	$0.8 + \frac{\pi}{100}$	41.33	6.0003	11.75	40.39	2.5468	5.06	40.10	1.7899	3.53
$\nu = 120$										
1.0	$0.2 + \frac{\pi}{100}$	123.92	18.6539	12.50	120.43	9.6798	6.42	120.67	7.4513	4.96
	$0.5 + \frac{\pi}{100}$	124.13	18.6797	12.28	120.79	9.1387	5.96	120.43	7.4005	4.79
	$0.8 + \frac{\pi}{100}$	123.24	18.5571	12.06	121.19	9.4779	6.29	120.30	7.3074	4.85
2.0	$0.2 + \frac{\pi}{100}$	124.36	17.6012	11.79	120.91	7.6146	4.98	120.31	5.4663	3.62
	$0.5 + \frac{\pi}{100}$	123.90	17.7542	11.80	120.81	7.6581	5.07	120.28	5.4583	3.65
	$0.8 + \frac{\pi}{100}$	122.80	18.1470	11.86	120.75	7.4617	4.97	120.31	5.6464	3.77
3.0	$0.2 + \frac{\pi}{100}$	123.39	18.1112	11.61	117.25	16.2003	7.67	115.25	18.7701	7.71
	$0.5 + \frac{\pi}{100}$	122.61	17.8808	11.84	118.15	14.9927	7.19	114.86	18.7331	7.58
	$0.8 + \frac{\pi}{100}$	121.77	17.7085	11.37	118.25	14.0907	6.71	114.12	20.3491	8.57
3.3	$0.2 + \frac{\pi}{100}$	122.96	17.5747	11.41	120.69	7.6545	5.07	120.74	5.4721	3.60
	$0.5 + \frac{\pi}{100}$	123.30	18.7992	12.36	120.78	7.7125	5.06	120.49	5.3755	3.57
	$0.8 + \frac{\pi}{100}$	124.71	18.6880	12.54	120.37	7.6214	5.10	120.38	5.2914	3.51

Table 5: Simulation Results for parameter θ considering Map 3, with θ assumed unknown, and sample size $n \in \{100, 500, 1000\}$: the mean estimated value of θ over 1,000 replications ($\bar{\theta}$), for $\nu \in \{10, 40, 120\}$, the standard deviation of the estimates (sd_θ) and the mean absolute percentage error (MAPE).

k	u_0	$n = 100$			$n = 500$			$n = 1,000$		
		$\bar{\theta}$	sd_θ	MAPE	$\bar{\nu}$	sd_ν	MAPE	$\bar{\nu}$	sd_ν	MAPE
$\nu = 10$										
1.0	$0.2 + \frac{\pi}{100}$	1.00	0.0057	0.45	1.00	0.0006	0.05	1.00	0.0002	0.02
	$0.5 + \frac{\pi}{100}$	1.00	0.0058	0.46	1.00	0.0006	0.05	1.00	0.0002	0.02
	$0.8 + \frac{\pi}{100}$	1.00	0.0056	0.44	1.00	0.0006	0.05	1.00	0.0002	0.02
2.0	$0.2 + \frac{\pi}{100}$	2.00	0.0579	2.29	2.00	0.0267	1.06	2.00	0.0185	0.74
	$0.5 + \frac{\pi}{100}$	2.00	0.0591	2.36	2.00	0.0263	1.03	2.00	0.0185	0.75
	$0.8 + \frac{\pi}{100}$	2.00	0.0603	2.39	2.00	0.0271	1.06	2.00	0.0189	0.76
3.0	$0.2 + \frac{\pi}{100}$	2.99	0.0503	0.83	3.00	0.0182	0.23	3.00	0.0141	0.14
	$0.5 + \frac{\pi}{100}$	2.99	0.0481	0.77	3.00	0.0182	0.23	3.00	0.0131	0.14
	$0.8 + \frac{\pi}{100}$	2.99	0.0480	0.82	3.00	0.0164	0.21	3.00	0.0114	0.13
3.3	$0.2 + \frac{\pi}{100}$	3.31	0.0546	1.27	3.30	0.0231	0.57	3.30	0.0165	0.39
	$0.5 + \frac{\pi}{100}$	3.30	0.0535	1.25	3.30	0.0233	0.56	3.30	0.0161	0.39
	$0.8 + \frac{\pi}{100}$	3.30	0.0536	1.27	3.30	0.0235	0.56	3.30	0.0161	0.39
$\nu = 40$										
1.0	$0.2 + \frac{\pi}{100}$	1.00	0.0039	0.31	1.00	0.0005	0.04	1.00	0.0002	0.02
	$0.5 + \frac{\pi}{100}$	1.00	0.0038	0.31	1.00	0.0005	0.04	1.00	0.0002	0.02
	$0.8 + \frac{\pi}{100}$	1.00	0.0038	0.31	1.00	0.0005	0.04	1.00	0.0002	0.02
2.0	$0.2 + \frac{\pi}{100}$	2.00	0.0311	1.23	2.00	0.0136	0.54	2.00	0.0097	0.39
	$0.5 + \frac{\pi}{100}$	2.00	0.0321	1.31	2.00	0.0140	0.55	2.00	0.0098	0.39
	$0.8 + \frac{\pi}{100}$	2.00	0.0311	1.24	2.00	0.0142	0.56	2.00	0.0099	0.40
3.0	$0.2 + \frac{\pi}{100}$	3.00	0.0126	0.25	3.00	0.0028	0.05	3.00	0.0027	0.03
	$0.5 + \frac{\pi}{100}$	3.00	0.0106	0.24	3.00	0.0022	0.05	3.00	0.0014	0.03
	$0.8 + \frac{\pi}{100}$	3.00	0.0114	0.24	3.00	0.0036	0.06	3.00	0.0018	0.03
3.3	$0.2 + \frac{\pi}{100}$	3.30	0.0279	0.67	3.30	0.0118	0.29	3.30	0.0090	0.22
	$0.5 + \frac{\pi}{100}$	3.30	0.0280	0.67	3.30	0.0115	0.28	3.30	0.0085	0.20
	$0.8 + \frac{\pi}{100}$	3.30	0.0265	0.64	3.30	0.0119	0.29	3.30	0.0087	0.21
$\nu = 120$										
1.0	$0.2 + \frac{\pi}{100}$	1.00	0.0024	0.20	1.00	0.0004	0.03	1.00	0.0002	0.01
	$0.5 + \frac{\pi}{100}$	1.00	0.0024	0.19	1.00	0.0004	0.03	1.00	0.0002	0.02
	$0.8 + \frac{\pi}{100}$	1.00	0.0025	0.20	1.00	0.0004	0.03	1.00	0.0002	0.01
2.0	$0.2 + \frac{\pi}{100}$	2.00	0.0191	0.75	2.00	0.0079	0.31	2.00	0.0059	0.23
	$0.5 + \frac{\pi}{100}$	2.00	0.0183	0.74	2.00	0.0083	0.33	2.00	0.0058	0.23
	$0.8 + \frac{\pi}{100}$	2.00	0.0184	0.74	2.00	0.0081	0.32	2.00	0.0057	0.23
3.0	$0.2 + \frac{\pi}{100}$	3.00	0.0049	0.13	3.00	0.0011	0.03	3.00	0.0007	0.01
	$0.5 + \frac{\pi}{100}$	3.00	0.0048	0.13	3.00	0.0010	0.03	3.00	0.0005	0.01
	$0.8 + \frac{\pi}{100}$	3.00	0.0050	0.13	3.00	0.0010	0.03	3.00	0.0005	0.01
3.3	$0.2 + \frac{\pi}{100}$	3.30	0.0165	0.40	3.30	0.0072	0.18	3.30	0.0053	0.13
	$0.5 + \frac{\pi}{100}$	3.30	0.0151	0.37	3.30	0.0068	0.17	3.30	0.0050	0.12
	$0.8 + \frac{\pi}{100}$	3.30	0.0163	0.40	3.30	0.0075	0.18	3.30	0.0051	0.12

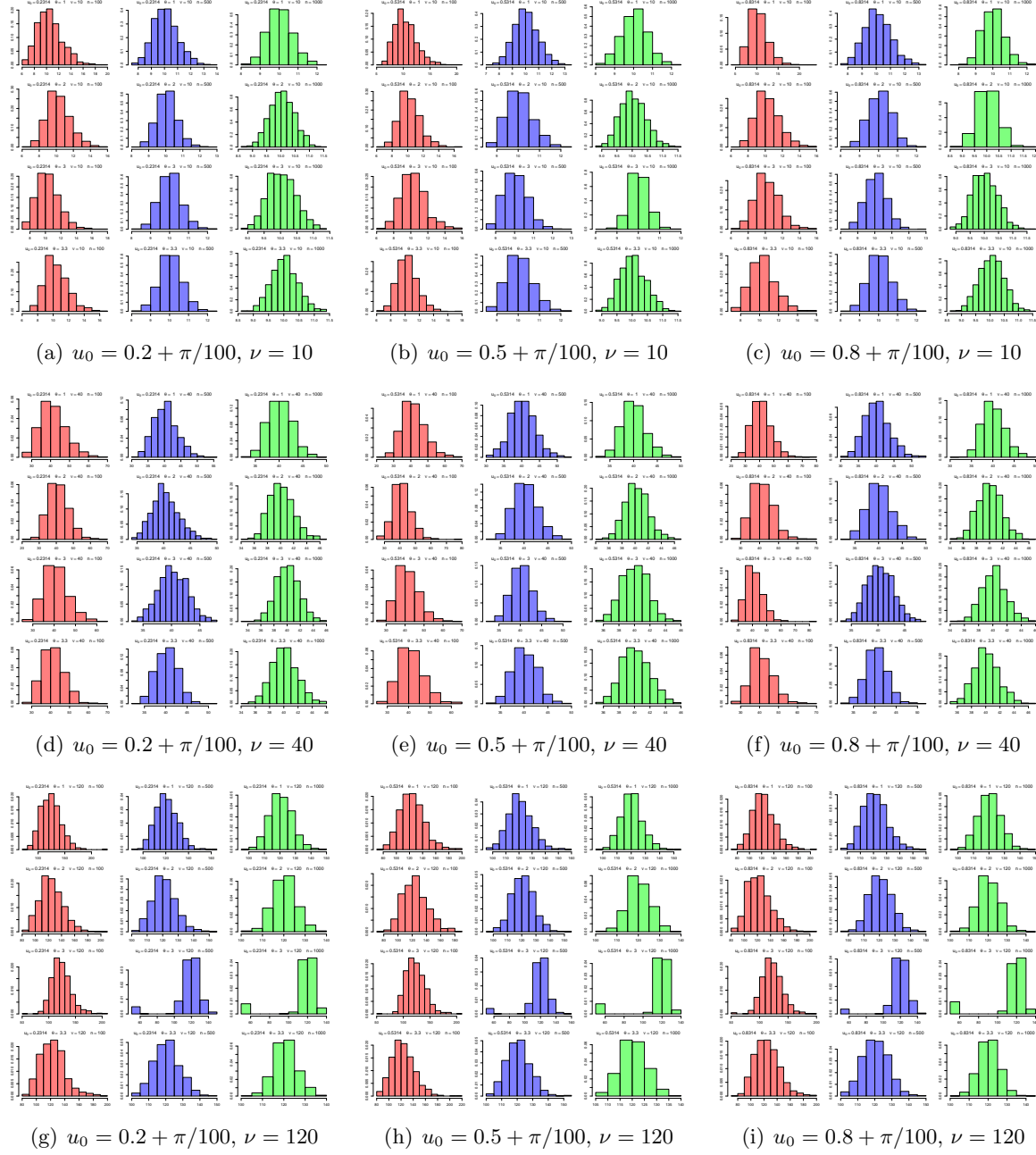


Figure 9: Histogram considering the estimated values, from 1,000 replications, for the parameter ν considering Map 3 with $\theta \in \{1, 2, 3, 3.3\}$ (respectively, from top to bottom in each subfigure) assumed unknown, when $n \in \{100, 500, 1000\}$ (red, blue and green, respectively).

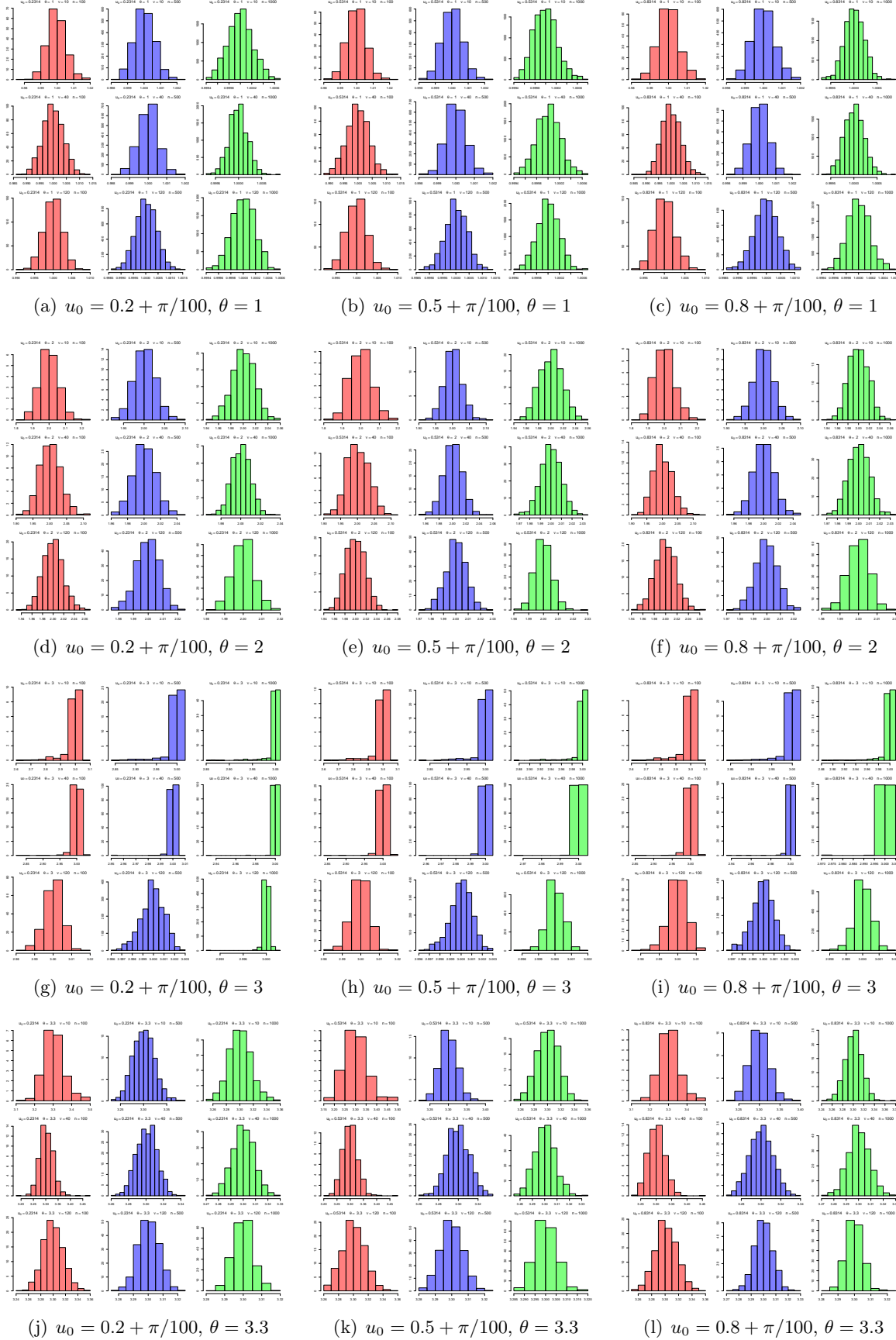


Figure 10: Histogram considering the estimated values, from 1,000 replications, for the parameter θ considering Map 3 with $\nu \in \{10, 40, 120\}$ (respectively, from top to bottom in each subfigure) assumed unknown, when $n \in \{100, 500, 1000\}$ (red, blue and green, respectively).

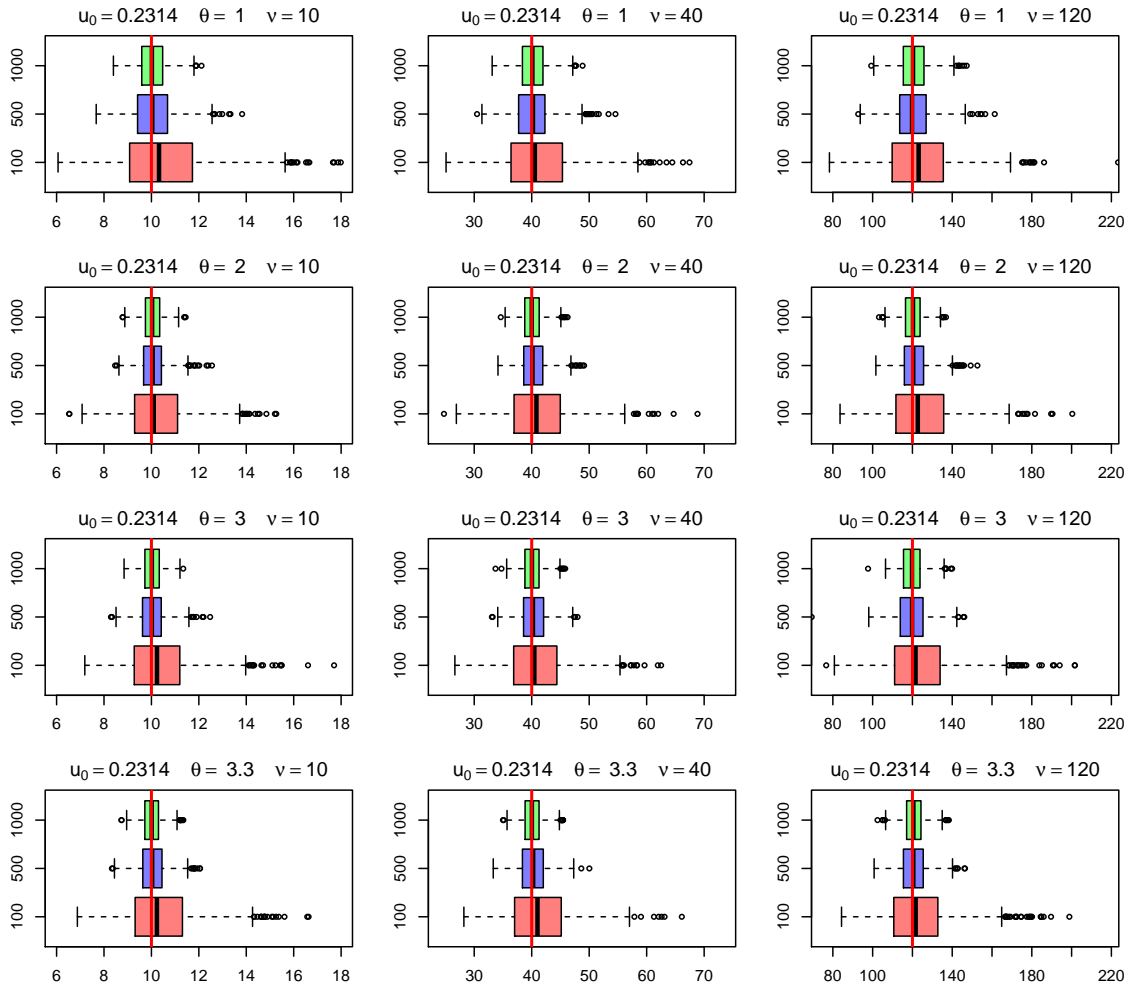


Figure 11: Simulation Results for the parameter $\nu \in \{10, 40, 120\}$ (from left to right) considering the Logistic Map with $u_0 = 0.2 + \pi/100$, when $n \in \{100, 500, 1000\}$ and $\theta \in \{1, 2, 3, 3.3\}$ (from top to bottom) is assumed unknown.

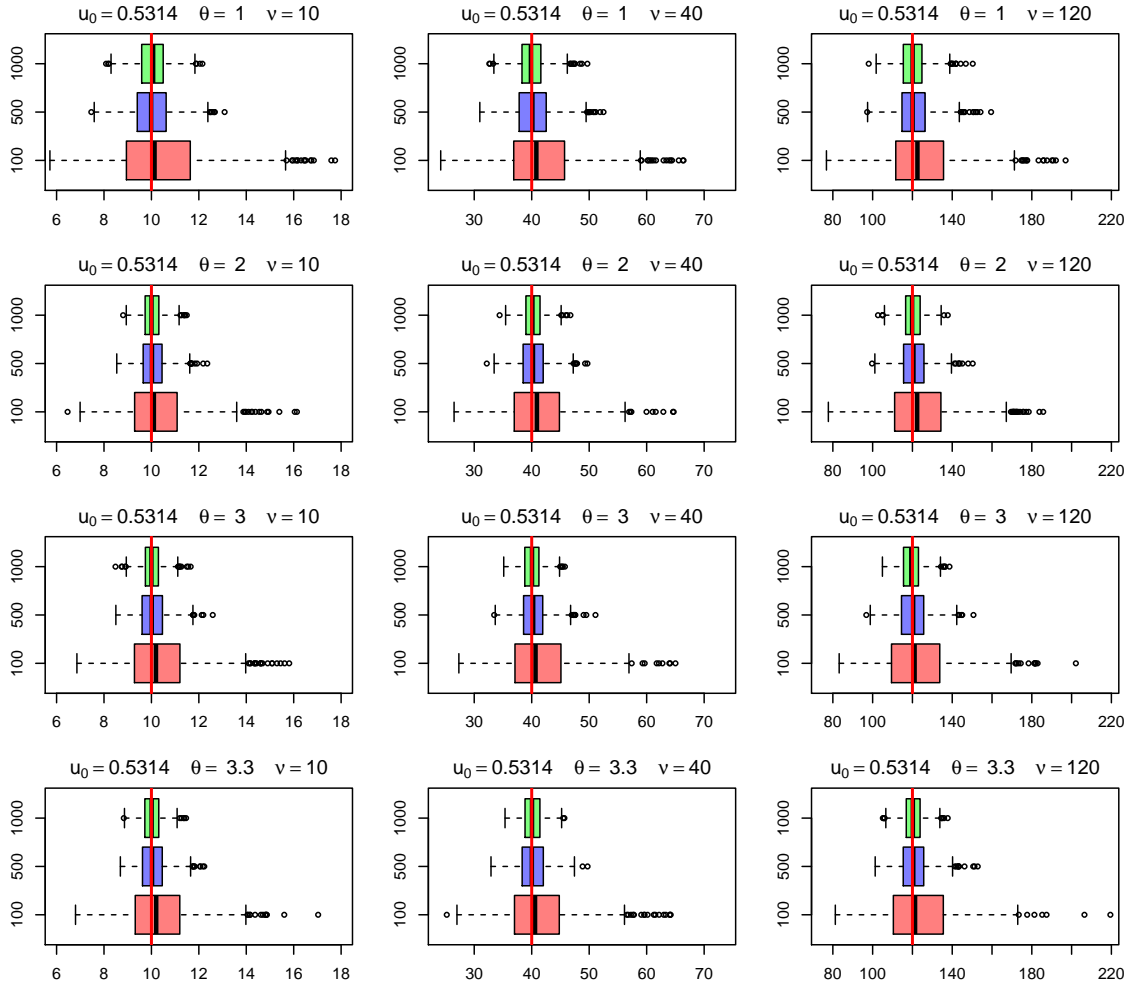


Figure 12: Simulation Results for the parameter $\nu \in \{10, 40, 120\}$ (from left to right) considering the Logistic Map with $u_0 = 0.5 + \pi/100$, when $n \in \{100, 500, 1000\}$ and $\theta \in \{1, 2, 3, 3.3\}$ (from top to bottom) is assumed unknown.

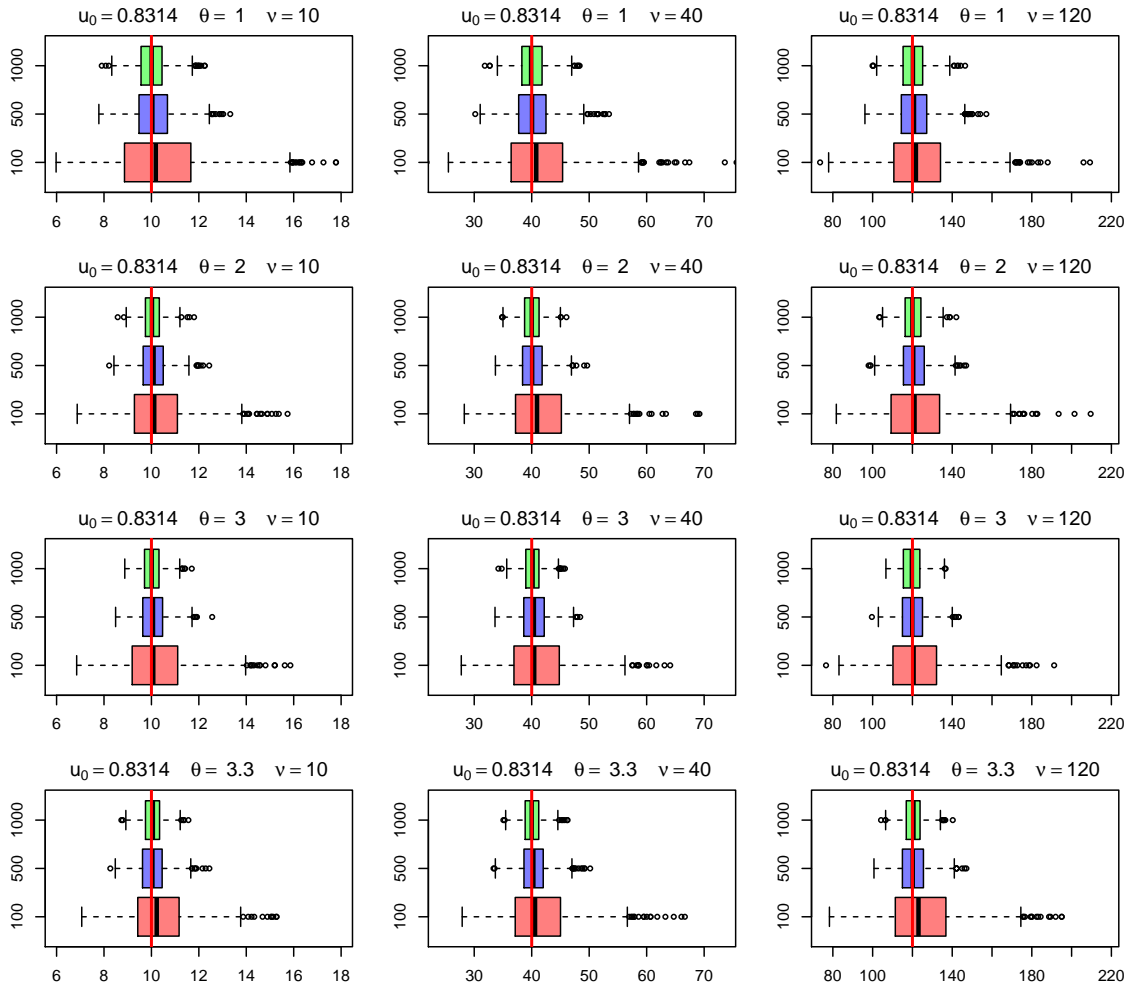


Figure 13: Simulation Results for the parameter $\nu \in \{10, 40, 120\}$ (from left to right) considering the Logistic Map with $u_0 = 0.8 + \pi/100$, when $n \in \{100, 500, 1000\}$ and $\theta \in \{1, 2, 3, 3.3\}$ (from top to bottom) is assumed unknown.

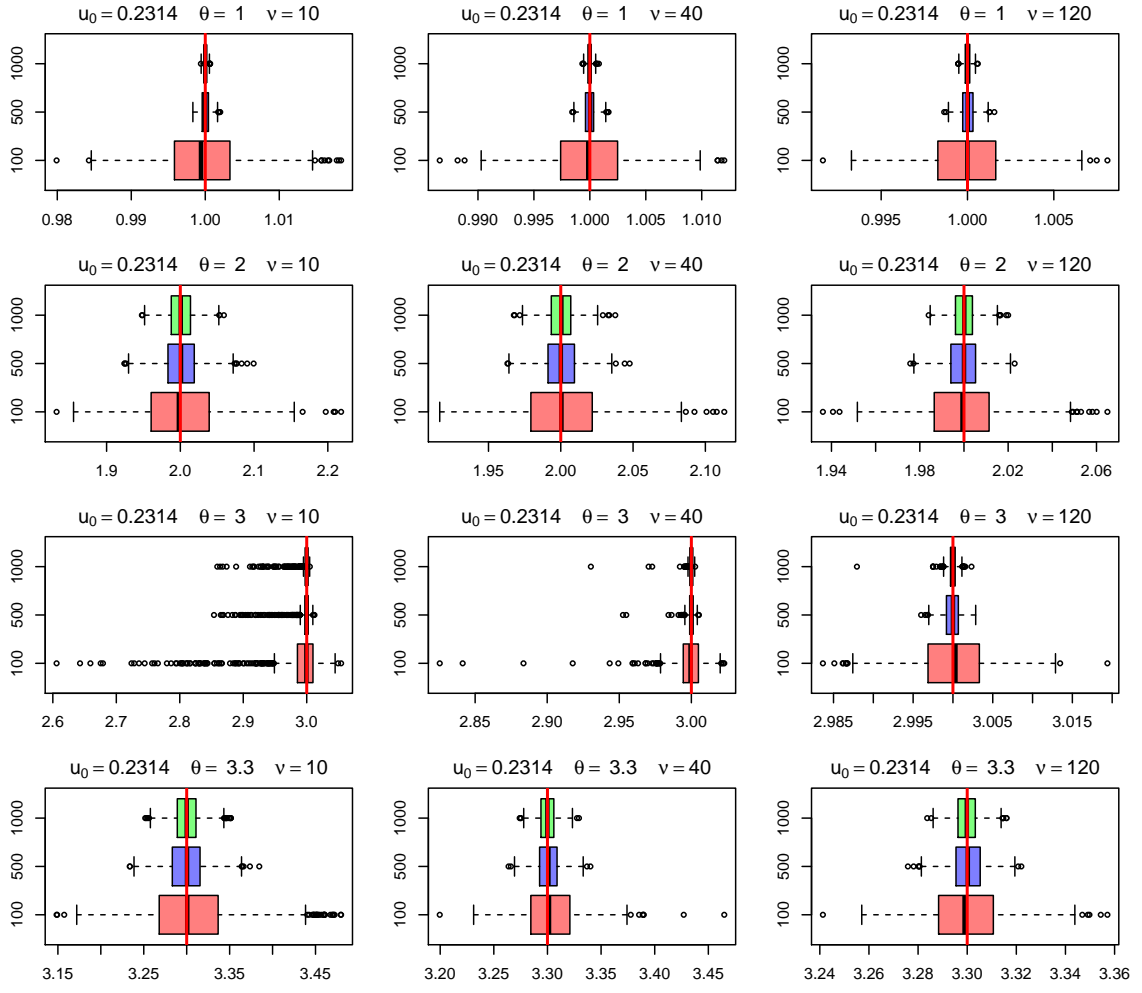


Figure 14: Simulation Results for the parameter $\theta \in \{1, 2, 3, 3.3\}$ (from top to bottom) considering the Logistic Map with $u_0 = 0.2 + \pi/100$, when $n \in \{100, 500, 1000\}$ and $\nu \in \{10, 40, 120\}$ (from left to right) is assumed unknown.

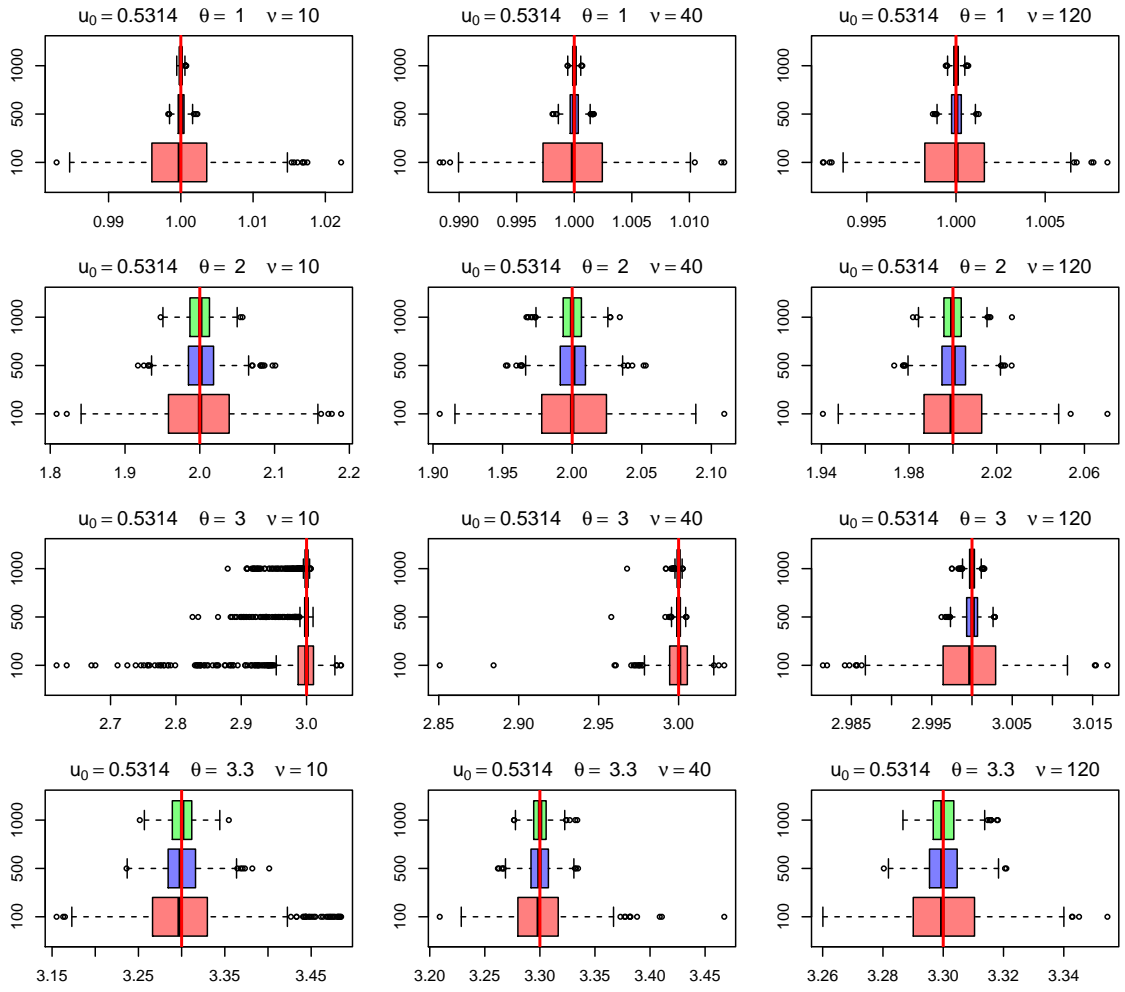


Figure 15: Simulation Results for the parameter $\theta \in \{1, 2, 3, 3.3\}$ (from top to bottom) considering the Logistic Map with $u_0 = 0.5 + \pi/100$, when $n \in \{100, 500, 1000\}$ and $\nu \in \{10, 40, 120\}$ (from left to right) is assumed unknown.

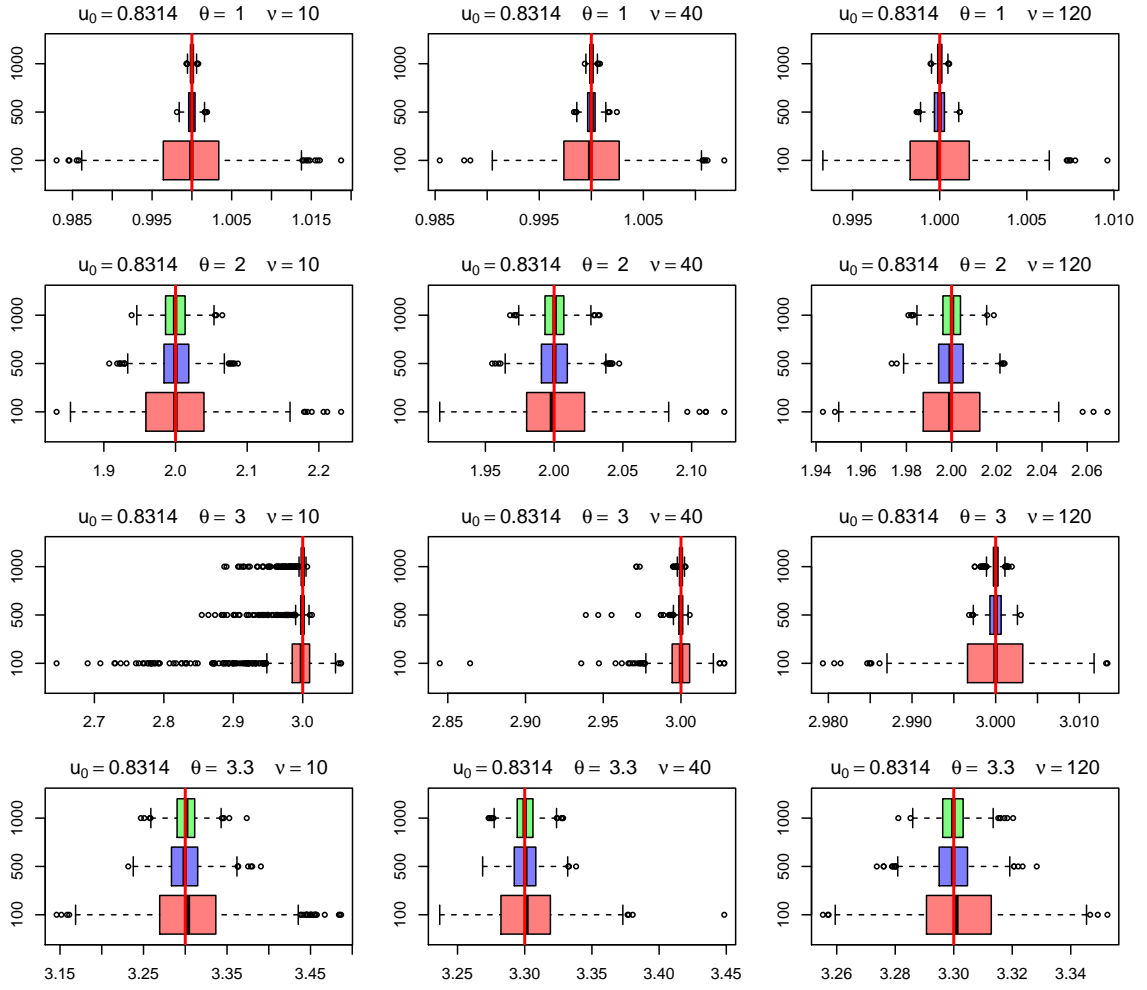


Figure 16: Simulation Results for the parameter $\theta \in \{1, 2, 3, 3.3\}$ (from top to bottom) considering the Logistic Map with $u_0 = 0.8 + \pi/100$, when $n \in \{100, 500, 1000\}$ and $\nu \in \{10, 40, 120\}$ (from left to right) is assumed unknown.